AD-A118 075 AIR FORCE INST OF TECH WRIGHT-PATTERSON AFB OH SCHOO--ETC F/G 1/2
DIRECT LIGHTNING STRIKES TO AIRCRAFT.(U)
JUN 82 J S SCHOWALTER
UNCLASSIFIED AFIT/GE/EE/82J-12 NL

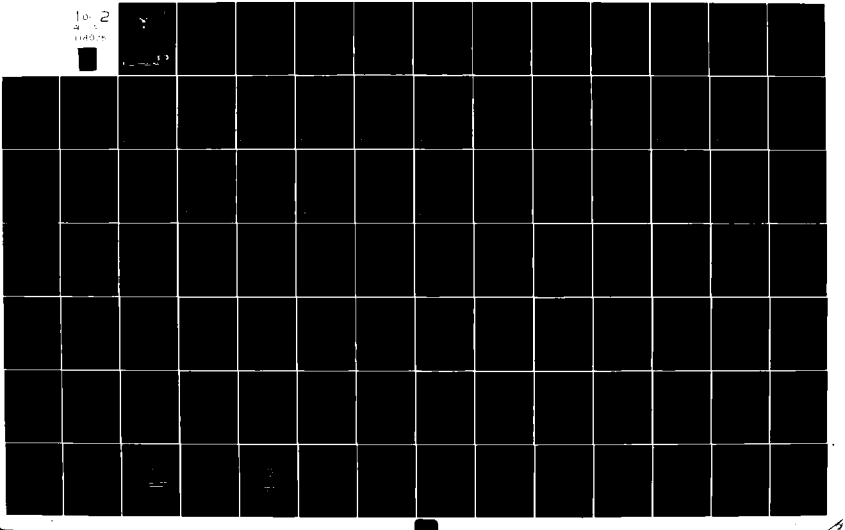

dde

(1)

AD A118075

DTIC FILE COPY

DTIC
ELECTE
AUG 11 1982
S D
E

DEPARTMENT OF THE AIR FORCE
AIR UNIVERSITY (ATC)

AIR FORCE INSTITUTE OF TECHNOLOGY

Wright-Patterson Air Force Base, Ohio

82 08 11 061

AFIT/GE/EE/82J-12

(1)

DIRECT LIGHTNING STRIKES TO AIRCRAFT

THESIS

AFIT/GE/EE/82J-12

JEFFREY S. SCHOWALTER
1st Lt USAF

Approved for public release; distribution unlimited

AFIT/GE/EE/82J-12

DIRECT LIGHTNING STRIKES TO AIRCRAFT

THESIS

Presented to the Faculty of the School of Engineering
of the Air Force Institute of Technology
Air University
in Partial Fulfillment of the
Requirements for the Degree of
Master of Science

by

Jeffrey S. Schowalter, B.A., B.S.
1st Lt USAF
Graduate Electrical Engineering

June 1982

Approved for public release; distribution unlimited.

Contents

Contents

Preface

During AFWAL's airborne lightning characterization program in the summer of 1981, the research plane experienced two direct strikes. My advisor, Capt. Pedro Rustan, had participated in the research program and thought an analysis of these direct strikes would definitely advance the state-of-the-art in this area. Until now such a detailed analysis of the electromagnetic environment during a direct strike had not been published.

Thanks are due to the personnel of AFWAL's Flight Dynamics Laboratory, Atmospheric Hazard's groups, especially Lt. Brian Kuhlman for his inputs into the data. Also thanks to the people at Technology Scientific Service Incorporated, T/SSI, especially Jean Reazer for her efforts on generating the computer plots of the data. Finally, Capt. Rustan's guidance and assistance were essential in the completion of this thesis.

List of Figures

List of Tables

Abstract

Two direct lightning strikes to a NOAA WC-130 aircraft equipped with eleven electromagnetic field sensors were recorded in South Florida during the summer of 1981. In both cases, the aircraft was flying in precipitation at an altitude of about 4 km and a few kilometers away from active thunderstorm regions.

An analysis of the data shows that both strikes exhibit a train of discrete pulses which can be correlated in most of the eleven sensors. The flashes lasted 295 and 460 msec and were characterized by an initial active period of about 40 msec with a pulse repetition rate of ten pulses per millisecond. In both flashes the most of the current flow was along the fuselage with peak currents estimated at 3 KA in one flash and 600 A in the other flash. A continuing current of an estimated 50 A was evident in only one strike. The electric field sensors recorded a maximum change of 200,000 V/M. In one flash the leader appears to propagate from the cloud to the aircraft with a duration of 350 μsec which implies a distance of about 175 m to the cloud charge center. In the other case the leader appears to initiate from the aircraft with a duration of about 188 μsec which implies a distance of about 100 m to the cloud charge center. No evidences were found of continued leader propagation after aircraft contact, thus suggesting the occurence of a cloud-to-aircraft lightning flash.

microsecond

Transients were measured on internal aircraft wires on the order of 40 mV. The largest pulses were induced on a wire which ran from wing to wing.

Introduction

Background

Lightning is one of nature's most spectacular phenomena and also one of the most dangerous, especially to aircraft. Many aircraft are struck by lightning each year with effects ranging from none at all to crashes with many lost lives. One of the most recent examples of lightning's potential for damage was the recent crash of an Air Force C-130E in South Carolina on November 30, 1978 (Ref.1). In this case, lightning struck the aircraft and caused the fuel tank to explode. Six lives were lost. This was just one of many crashes that can be attributed to lightning.

One of the biggest problems that faces the designers of aircraft is the lack of understanding of lightning's interaction with the aircraft. There is an urgent need for this type of data. Today's market demands all-weather capabilities for aircraft and thus an increased chance of encounters with lightning. The problem of designing aircraft to withstand these encounters is large especially since there has been little data collected on what conditions to expect. The problem is compounded by the fact that computer systems are being installed on aircraft and the newest skin composites are non-metallic. The computer boom has hit the aircraft industry as hard as any other sector of modern society. Sophisticated high speed-low power electronics systems are especially vulnerable to the

sub-microsecond risetime induced fields that lightning can produce. Not only must the aircraft designers worry about protection from direct lightning strikes but he must also worry about near-field effects.

The new non-metallic skins proposed for aircraft also add a new wrinkle. Fuel efficiency has prompted a call for these new lightweight non-metallic materials. These materials will lessen the degree of protection that metallic skins now enjoy. The metallic skins act essentially as perfect conductors and thus keep most lightning currents flowing on the skin shielding of the internal components. Non-metallic components on aircraft (such as radomes) have always been much more susceptible to damage than their metallic counterparts. More non-metallic areas on aircraft suggest the possibility of greater damage unless appropriate protective techniques can be found.

The present state-of-the-art on aircraft interaction with lightning is limited. Most of the present aircraft were designed for protection from lightning based on ground measurements of lightning characteristics. Since this is not the aircraft's primary environment, this data has limited usefulness. There have been several attempts to collect lightning data on board aircraft starting with Gunn (Ref.2) in 1948, Fitzgerald (Ref.3) in 1968, Nanevicz (Ref.4) in 1977, the French (Ref.5) in 1979, NASA (Ref. 6 and 7) in 1980-81 and finally AFWAL (Ref.8, 9, and 10)

in 81-'2. Some information has been obtained as to the fields and currents that can be expected on board aircraft. A further discussion of present knowledge on airborne lightning data is contained in a later chapter.

Presently only two groups are collecting airborne lightning data. NASA (Pitts) has had a project on-going for several years using a F106 as the research aircraft where 20 direct strikes have been reported. Most of the data has yet to be analyzed. The USAF Wright Aeronautical Laboratories (AFWAL) have just finished a three year (1979-81) airborne lightning characterization program. A WC-130 aircraft was instrumented with wide band electromagnetic field sensors and was flown in close proximity to active thunderstorms to record the characteristics of the electric and magnetic fields in the aircraft environment.

The data used in this thesis is the direct strike data collected by AFWAL during the summer of 1981. Direct strikes to the aircraft occurred in two different flights. The first direct strike occurred on the 17th of July and the second strike occurred on the 26th of August.

Approach

The presentation of these two direct strikes is as follows: first a look is taken at some of the literature in the field of airborne direct lightning strike research. Gunn (Ref. 2), Fitzgerald (Ref. 3), Nanevicz, et al (Ref. 4), the French Transall data (Ref. 5), NASA (Ref. 6 and 7) and

AFWAL (Ref. 8, 9, and 10) discuss the subjects of airborne collection and characterization of direct lightning strike data based on experimental values. Pierce (Ref. 11), Shaeffer (Ref. 12), Clifford (Ref. 13), and Clifford and Kasemir (Ref. 14) present theoretical approaches to the triggering of lightning strikes by aircraft.

Next the instrumentation of the aircraft used in this research is explained. Included is a discussion on the sensors used along with some of the theory behind the sensor design. The configuration used to mount the sensors and data processing involved in the production of results is also discussed.

After the instrumentation is discussed, the two direct strikes are analyzed. The data is presented by means of a look at several different time scales. The data windows range from 800 msec to 164 μs. An analysis of the data is then made for each of the two strikes by looking at the data in consecutively smaller time windows. Characteristics of the events at each of these data windows are discussed. A comparison is made of this direct strike data to past direct strike data that has been presented by Fitzgerald (Ref. 3), Nanevicz (Ref. 4), the French (Ref. 5), NASA (Ref. 6 and 7) and Rustan (Ref. 8) are pointed out.

A model that simulates the direct strikes is then developed. This is a rather simplified model, however, most of the important characteristics of the flash are present.

Finally some recommendations and conclusions are presented that were derived from this data. It is hoped that this section will aid future research in this area in pointing out some of the problem areas encountered as well as areas that need more research before conclusions can be reached.

Literature Review

General

The purpose of this chapter is to summarize, in chronological order, the research that has been done in the area of direct strikes to aircraft. Both experimental research and theoretical research are investigated. Actually little research has been done in this area. There are three basic factors that are involved in the lack of research in this area. First, aircraft measurements of lightning are dangerous. Lightning is very unpredictable and many times the accompanying weather is also a hazard to the aircraft. Secondly, until recently the electronics that needed to be aboard a lightning research aircraft were cumbersome and were not sensitive to fast field changes. Finally the research is expensive. There is the cost of specialized technical equipment as well as the cost of flying the aircraft. These factors combine to essentially leave the task of lightning research up to the federal government, even though this has actually been the case since airborne lightning research began.

Gunn 1948

The first published airborne lightning research was in 1948 by Gunn (Ref. 2). The purpose of this research was to measure the static electric field on the surface of aircraft flying through clouds. The aircraft used in this project consisted of a B25 medium bomber and a B17

medium bomber. The main instrumentation used in this project was the electric field meter that measured the electrostatic field. These electric meters were mounted on the belly and on the top of the fuselage just aft of the main wing. The meters measured the sign of the electric field and were calibrated to measure fields up to 100, 400, 1000, 4000 volts/cm depending upon scale selection. This particular configuration enabled Gunn to determine the magnitude of the vertical electric fields produced by the clouds outside the airplane. The electric field caused by the accumulation of free charge on the airplane itself produces a radically directed field. The electric field produced by the cloud is a vertically directed field. At the two sensor locations the field produced by the aircraft either adds or subtracts from the cloud field so that the relative contributions of both these fields can then be determined.

Gunn then presented the electric field data from fair weather clouds and thunderclouds. The flights encountered all types of weather including three direct strikes. Some of the data presented was one of the direct strikes. He reported a value of 340,000 V/M just prior to the instant of discharge on the belly sensor.

The main conclusion reached by Gunn was that just prior to a lightning discharge, the static electric field is on the order of 300,000 V/M, based on the three direct strikes.

Fitzgerald 1968

The next research project was reported on by Fitzgerald in 1968 (Ref. 3). This research was conducted from 1964-1966 and used several aircraft. C130, F100F, and U2 aircraft were instrumented and flown in the vicinity of Florida thunderstorms. He classified his results into two categories: a triggered lightning strike or a static discharge. Fitzgerald presents mostly statistics on strikes but also includes some data. The most interesting data presented concerns the currents recorded on high-frequency oscilliscopes. However, the upper limit on this frequency response is not mentioned. This data is reproduced in Table I.

Sensor Location	Number of Measure-ments	Peak Current-(Kamperes)	Peak Rise Time A/μS	Peak Fall Time A/μS
Nose Boom	30	5.8	2000	7000
Right Wing Tip	19	14.5	5000	2200
Left Wing Tip	4	2.8	----	----
Vertical Stabilizer	23	22.0	2000	210

Table I Fitzgerald Data Summary

He also points out that a feature of the in-cloud strikes was a high repetition rate; restrikes occurred at intervals of a millisecond or two in some areas. This is characteristic of the direct strike data presented here and will be discussed after the analysis of the direct strikes. He also measured electrostatic fields using a system of induction field meters similar to those used by Gunn (Ref. 2). At the time of the strike, the highest static electric field was 390,000 V/M. Charge on the aircraft was determined based on the electric field produced by the aircraft. However only a breakdown of high, medium, or low charge present before a strike is tabulated. A quantized catagory breakdown would have been more helpful in determining how our estimates of charge compare with those recorded by Fitzgerald.

Shaeffer 1972

An article on aircraft initiation of lightning was written by Shaeffer in 1972 (Ref. 12). This paper, based on analytical results and lightning simulation testing, indicated that aircraft could indeed trigger lightning.

The article started with a summary of statistics on lightning strikes to the F-4. Next he discussed the physical mechanism needed to initiate breakdown. By use of the method of moments, the intensification of the electric field was determined for different points on the aircraft. Shaeffer stated that the points of highest intensification

correlated well with usual lightning attachment points. Although the field is large enough to initiate breakdown, Shaeffer states that the charge on the aircraft will only support slight streamering unless there is an external source of charge. He does not however state exactly how much streamering the aircraft produces or the charge magnitude necessary to produce a leader.

Jet engine exhaust test are then presented and shown not a significant factor for lightning initiation since they have relatively low conductivity. Finally laboratory lightning mechanism tests were performed to investigate various breakdown mechanisms. A sphere was placed between two disk electrodes and parameters such as charge and position were varied. The greatest effect was seen when the sphere was varied in position in the gap. The main conclusion reached by Shaeffer was that an aircraft can support streamer initiation if an external source of charge is present and if the electric field at some point on the aircraft exceeds the breakdown of free space.

Pierce 1972

Pierce, 1972 (Ref. 11) discussed two cases of triggered lightning. The first was the case of triggered lightning for objects that come in contact with ground. His suggestion was that the voltage discontinuity created by the length of the object intensifies the field to trigger lightning. Tall buildings, rockets or depth charges are documented examples.

In the second case, Pierce discussed triggering of lightning by objects in flight. He describes the best known triggered lightning incident of the Apollo spacecraft (Ref. 20). Pierce stated that the length of the spacecraft was augmented effectively by a conducting exhaust fume. Pierce developed two criteria so as to indicate necessary and sufficient conditions for triggered lightning; (1) a general ambient field of some 10 KV/M and (2) a local potential discontinuity for aircraft was probably due more to charge on the aircraft than the ambient field and the aircraft dimension.

Nanevicz et. al. 1977

Airborne lightning measurements were presented by Nanevicz, et. al. (Ref. 4) in 1977. The measurements were taken from a Lear jet during the summer of 1976. A ten channel spectrum analyzer was used. Four of the channels generated signals induced in an electric dipole antenna on the top of the fuselage with responses at 1, 3, 10, and 30 MHz and bandwidths of 20 KHz each. Four channels recorded the short circuit currents induced in the wire on the roof of the interior fuselage. Another channel recorded the vertical component of the electrostatic field. A final channel recorded the response of a 10 KHz tuned circuit coupled to the electrip dipole antenna.

The most relevant data presented was the direct lightning strike on 10 August 1976. The aircraft was just

outside of a cloud at an altitude of 37,000 feet (9 km), when it was struck by lightning. The stroke attachment points were the nose radome and the aft end of the right wing fuel tank. The nose radome was damaged enough to be replaced and the fuel tank was burned and pitted. No mention was made however of the depth of the pit marks caused by the swept stroke. The flash lasted about 0.7 sec and was characterized by two main bursts of pulses with a pulse repetition rate of about 0.2 pulses per millisecond. The first burst occurred at the beginning of the flash and lasted for about 40 msec. This time period agrees with our data for the most active period of both flashes analyzed in this thesis. Then after a 25 msec quiet period, the second burst of pulses continued for another 25 msec. Maximum electric field change was about 50,000 V/M. The highest amplitude pulses showed no identifiable relationship between spectral components. Furthermore, the amplitudes of the wire pulses showed no systematic relationship to the dipole antenna pulses. Comparisons to a laboratory applied current step inferred a current in excess of 1 A flowing in the cabin wire. Other activity seen in the electric field sensors was attributed to isolated K-changes. A comparison of the Lear jet direct strike data was made with a model of an intracloud flash developed by Cianos and Pierce (Ref. 18). The results of the analysis are displayed in Table II.

	Total Duration	K-changes	Average Interval Between Pulses
Lear jet	700 ms	40	17 msec
Model	200 ms	30	6 msec

Table II
Comparison of Lear Jet Strike With Intercloud Model

The average interval between pulses for the Lear Jet strike is almost three times larger than the model and the "bursty" pulse characteristic of the Lear jet strike cannot be explained by the model.

French Transall Data 1978

The French conducted airborne lightning research in 1978 using a Transall C-160 aircraft. Thirteen strikes to the aircraft were recorded with most occurring in clouds in mixed ice and rain at temperatures between 0^{o} and $-5^{o}C$. The direct strikes were classified into three arbitrary catagories. The first catagory of six strikes was characterized by peak currents less than 4.5 KA. Total number of pulses were 3 to 12 with each pulse lasting 8 to 200 μsec. Maximum continuing current was less than 2 KA. The second catagory of three strikes has a single pulse of less than 70 KA and a pulse duration of 80 to 200 μsec. The continuing current was less than 500 amps. The third catagory of four strikes had two groups of up to 8 pulses with a peak current of less than 50 KA. Each pulse was between 20 and 200 μsec and the two groups of pulses were

50 msec to 14 msec apart. All strikes had a continuing current base.

The following table summarizes the maximum current and current charges seen in each of the direct strikes.

Event	Maximum Current (KA)	Maximum $\frac{dI}{dt}$ (KA/μS)
1	15	2
2	2.5	.1
3	28	.5
4	45	6
5	14	1
6	4	.1
7	3.5	.3
8	50	4
9	4	.06
10	8	.07
11	3	.1
12	70	26
13	6	.3

Table III French Transall Data Summary

Current was measured using two four meter rods placed at each end of the aircraft. The rods were instrumented using a coaxial shunt with a 1 MΩ resistor which had an 80 nsec response. The peak currents of 45-70 KA are except-

ionally high even for cloud-to-ground flashes and might be attributed to instrumentation errors.

Clifford 1980

Clifford, in 1980 (Ref. 13), reviewed some basic thoughts about aircraft triggered lightning. He summarized some of the meteorological statistics and conditions during lightning strikes. The most predominant conditions reported for a direct strike are $0^{o}C.$, in cloud with mixed precipitation and in light turbulence. Next Clifford looked at the mechanisms or processes that would be necessary for a static discharge to occur by first discussing tribo electric charging. The precipitation charging current is given by

$$i = p\ c\ v\ A_{eff}$$

where

p = charge per particle

c = particle concentration

v = aircraft velocity

A_{eff} = effective intercepting area of aircraft

He states that this calculation yields total aircraft charging currents of a few hundred microamp, although values as high as three milliamps have been measured in flight. However, this charging rate is too low to produce a static discharge and Clifford postulates that extremely high charging rates may rarely occur although none of these high rates have ever been measured.

Another mechanism Clifford suggests is that the wake of the aircraft may extend the effective length of the aircraft and thereby increase the voltage discontinuity and thereby initiate a discharge. However the aircraft must be aligned with the ambient field before the electric field will intensify. Finally he states that continuing research must be done in the area of triggered lightning.

NASA 1981

Another effort to collect in-flight lightning strike data was made by NASA and reported by Trost & Pitts (Ref. 7) and Pitts (Ref. 6). The data collected for this program is of 20 direct strikes from the summers of 1980 and 1981. The research aircraft was an F-106B. The sensor types were as follows: nose boom current (I) and its rate of change (I-Dot), rate of change of electric and magnetic flux density (D-Dot and B-Dot) and static electric field (E). The I and I-Dot were located at the base of the nose and the D-Dot sensors were located under the fuselage, under the wings and on the port side of the vertical fin. B-Dot sensors were located at opposite sides of the aft fuselage and under the wings. E sensors were located near the nose and configured to measure Ex, Ey, and Ez. The easiest was to summarize their results is by use of the tables below adapted from Trost and Pitts, 1981.

	D-Dot	B-Dot	I-Dot	I	I-Dot (Estimated from B-Dot)	I-Dot (Estimated from I
Sensor Location	Fuselage	Fuselage	Nose Boom	Nose Boom		
Max Peak-Peak Value	30.8A/M	1160T/S	0.72KA/μS	14KA	22KA/μS	12KA/μS
Sample Interval	10ns	10ns		16.7ns		
BW	50 MHz	50 MHz	6 MHz	30 MHz		

Table IV Summary of Peak Values

In addition the characteristic of one of the strikes is presented. This strike occurred at 33,000 feet on September 3, 1980. The complete event consisted of over 100 pulses spread in time over a period of 760 msec. Some numerical values are given below.

Peak Value	H = 5.6 A/M E = 380 KV/M I = 88A	
Rise Times	H	21 ns
	E	690 ns
	I	(bandwidth limited) 410 ns

Table V

Characteristics of Fields During 3 Sept. 80 Strike

In addition aircraft resonances are discussed. It is concluded that the data correlates well with the resonances identified on a scale model of the F-106. The lowest resonance corresponds to the fuselage half-wave length resonance. However this model does not simulate actual flight conditions and these resonances are based on frequency domain plots of individual pulses rather than an entire flash.

AFWAL

Recent work which is fully related to this research is the AFWAL program reported by Baum (Ref. 9) and Rustan et. al. (Ref. 8 and 10). Baum summarized the instrumentation package used the first year of the project. He also introduced some of the techniques used to determine aircraft coupling. Finally he presented some of the general wave forms that had been recorded. Rustan et. al. reported

the data collected all three years. They described the instrumentation as well as correlation with ground data. The direct strikes reported in this thesis were briefly analyzed. There was no correlated ground data for the direct strikes. Some of the conclusions reached about the direct strike data were as follows:

1) There is no evidence that the strike made a ground contact.

2) Streamers propagated between the aircraft and the cloud producing the flash.

3) The risetimes of the electromagnetic field pulses and induced transients were not less than about half a microsecond.

4) The flash induced a 50 mV transient on the fuselage wire and this was the expected cause of a computer failure experienced on board the aircraft.

Clifford and Kasemir 1982

One of the most recent articles on triggered lightning was presented by Clifford and Kasemir (Ref 14). The purpose of this paper was to review the evidence and arguments for aircraft-triggered lightning drawing upon ground-based triggered data for insight into the triggered process. They begin with a discussion of ground based triggering citing several examples. Triggered lightning is defined as having an upwards moving leader while natural lightning has a downwards moving leader. Next rockets are discussed which also trigger (upwards moving leader) lightning. It is stated that the voltage discontinuity required to trigger a flash by a rapidly

moving rocket should be somewhat less than for stationary structures. They cite calculations by Brook that show if the relative velocity between air and a point is greater than the ion drift velocity (about 100 m/sec), the screening space charge cannot develop, thereby shielding from the cloud does not take place.

For non-grounded triggering Clifford and Kasemir cite several examples of non-grounded triggering and state that for the airborne case, Pierce's expression for voltage discontinuities should be

$$V = \tfrac{1}{2} \int_0^L \bar{E} \cdot \overline{dl}$$

where

$\bar{E}$ is cloud field vector
$\overline{dl}$ is length element along object

The factor of $\frac{1}{2}$ comes from the fact that the potential at the midpoint of the conductor must be zero, thereby length decreases by one half of the grounded case. They expect voltage discontinulties as low as 500-750 KV as adequate to trigger lightning from airborne systems under optimum conditions.

Clifford and Kasemir then survey some of the in-flight lightning strike articles, most of which are presented in this thesis. The main conclusion reached from this survey is that aircraft do trigger lightning in clouds that have produced no natural lightning.

Next a discussion on lightning triggering concepts is presented. First enhanced field breakdown processes are explored. Some sources are cited that indicate that there is no set threshold electric field value that will guarantee a strike. Aircraft wake enhancement factors are also presented as a possible source of inconsistent electric field measurements.

Finally the characteristics of a triggered strike are examined. A continuing current of a few hundred up to several thousand amps is expected to last tens to hundreds of milliseconds. There may also be several discrete pulses of moderate to low amplitude (2 to 50 KA) with risetimes of several microseconds. Possibly a single high amplitude discharge with a risetime of tens of microseconds may be encountered. Damage done by a triggered strike can produce serious damage.

Several articles have been reviewed here. They fall into two broad catagories. The first catagory of articles is experimental research. Gunn (Ref. 2), Fitzgerald (Ref. 3), Nanevicz, et. al. (Ref. 4), the French (Ref. 5), NASA (Ref. 6 and 7), and AFWAL (Ref. 8, 9, and 10) constitute the major efforts in the area of airborne lightning research. The second catagory of articles is theoretical. Pierce (Ref. 11), Shaeffer (Ref. 12), Clifford (Ref. 13), and Clifford and Kasemir (Ref. 14) are based on laboratory studies and correlation between research articles. Con-

clusions and hypotheses are then drawn from data.

These articles are directly related to airborne lightning research and aircraft triggered lightning. There have been many other articles written that are indirectly related to these areas. The references in Clifford (Ref. 13) and Clifford and Kasemir (Ref. 14) serve as a good background starting point for related articles.

Instrumentation

This data was collected in the last year of a three year program on lightning characterization. This three-year program was evolutionary. The first year a fairly simple system was used and a small amount of useful data was obtained by R. Baum, (Ref. 9). The main emphasis during the first year was to capture data windows of 2048 points of the largest electric and magnetic field radiation incident upon the aircraft between 5 and 20 km of the lightning flash. For this purpose, four aircraft sensors were designed and the interface instrumentation was developed. A new system was implemented during the second year and sufficient data was collected to analyze system performance. During the second year, the number of aircraft sensors was increased from 4 to 11.

During the third and final year additional changes were incorporated to obtain a consistent set of airborne data. The WC-130 aircraft used during this final year was instrumented with 11 sensors to measure the electric and magnetic field external to the aircraft and the current density on the external skin of the aircraft. In addition, two internal wires were run, one along the trailing edge wing of the left wing box and the other in the fuselage nose-to-tail to measure induced transients. The sensors were mounted on the aircraft as shown in Figure 1. The D-Dot sensors are referred to by location as follows:

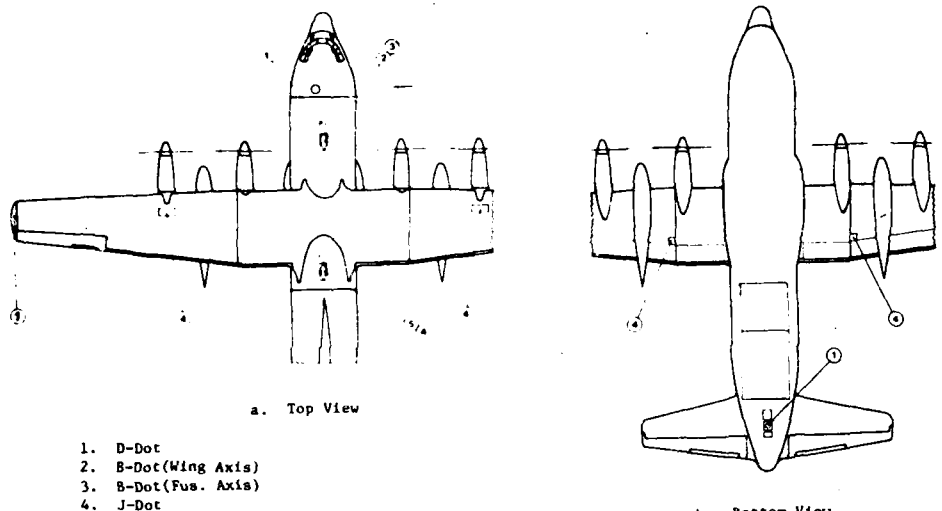

a. Top View

b. Bottom View

1. D-Dot
2. B-Dot(Wing Axis)
3. B-Dot(Fus. Axis)
4. J-Dot
5. Q-Dot

Figure 1 Sensor Locations

front upper fuselage (FUF), left wing tip (LWT), and aft lower fuselage (ALF). The B-Dot sensors were oriented to be sensitive to B field corresponding to either current flow nose to tail (NT) or current flow from wing to wing (WW). The J-Dot sensors located on the wings are sensitive to current flowing to wing and are referred to by location; right upper wing (RUW), right lower wing (RLW), left upper wing (LUW), and left lower wing (LLW). There is also a J-Dot sensor located on the fuselage sensitive to current flow nose-to-tail and is referred to by location; aft upper fuselage (AUF). The Q-Dot sensor was located at the aft upper fuselage (AUF).

Three basic types of sensors were mounted on the aircraft: electric field sensors, magnetic field sensors and current density sensors. The principles of operation of the sensors are based on Maxwell's equations. These sensors were developed for work in the area of emp. Since the direct strike data was collected using Electric Field, Magnetic Field and Current Density sensors, a description of these sensors is now presented.

Electric Field Sensor

A dipole sensor was used to measure the vertical component of the incident electric field. Two models of this sensor were used; a flush plate and a spherical referred to as D-Dot and Q- Dot respectively. The choice depended upon the amount of curvature at the point where the sensor

was mounted. These models were used in an effort to best measure incident electric field.

Figure 2 shows the basic configuration. The electric field perpendicular to the plates induces a voltage between the plates. Figure 2b shows all the basic circuit elements in the sensor. C and G represent the capacitance and conductance between the parallel plates. The stray capacitance C_s at the sensor output and the line resistance are also considered in the electric field sensor equivalent circuit in figure 2b. The sensor output is matched to a 50 ohm line. In air, the conductivity between plates will be about 10^{16} siemens/cm and a typical value for C is about 1pFd. Therefore, G can be neglected over the entire frequency range. In addition, the line resistance R is negligible with respect to the load. Figure 2c shows the remaining elements. The sensor current can be determined using the Norton equivalent circuit in figure 2d.

$$I_{in}(w) = V_{in}(w)\ jwC = jwC\ d\ E(w) \qquad (1)$$

Where E(W) is the electric field sensed between the plates and d is their separation. But since the capacitance between the plates is

$$C = \epsilon_o A/d \qquad (2)$$

where A is the plate area, substituting (2) in (1) we get

$$I_{in}(w) = \epsilon_o A\ E(w). \qquad (3)$$

Defining $C_1 = C + C_s$, the equivalent circuit in figure 2 d is obtained. Therefore, (4)

$$V_{in}(w) = I_{in}(w)/wC_1 = (\varepsilon_o A/C_1)\, E(w) = d'\, E(w) \quad (5)$$

where, as expected, the input voltage between the plates is proportional to the electric field and d' is the equivalent plate separation (.101 m). The equivalent sensor capacitance C_1 was calculated to be 7.1 pFd (Ref. 15).

From figure 2e the output voltage V_{out} can be calculated as:

$$V_{out}(w) = \{R_L/(R_L + 1/jwC_1)\}\, V_{in}(w) = \{jwR_LC_1/(1 + jwR_LC_1)\}V_{in}(w)$$
$$= \{jwR_L\, \varepsilon_o A/(1 + jwR_LC_1)\}\ E(w) \quad (6)$$

Two extreme cases can be observed from equation (6). first, for $w << 1/R_LC_1$ then

$$V_{out}(w) = jwR_L\varepsilon_o A\ E(w) \quad (7)$$

which implies that the measured voltage is proportional to the derivative of the electric field. Second, for $w >> 1/R_LC_1$ then

$$V_{out}(\omega) = (\varepsilon_o A/C_1)\, E(\omega) = d'E(\omega) \quad (8)$$

where the measured voltage is proportional to the electric field.

Since R_L = 50 ohms, C_1 = 7.1 pFd, and $1/2\pi R_LC_1$ = 447 MHz, over the frequencies of interest $\omega << 1/R_LC_1$ and the output voltage is always proportional to the derivative of the electric field.

In the time domain, $V_{out}(t) = \varepsilon_o A\ R_L \frac{dE(t)}{dt} = K_E \frac{dE(t)}{dt}$ (9)

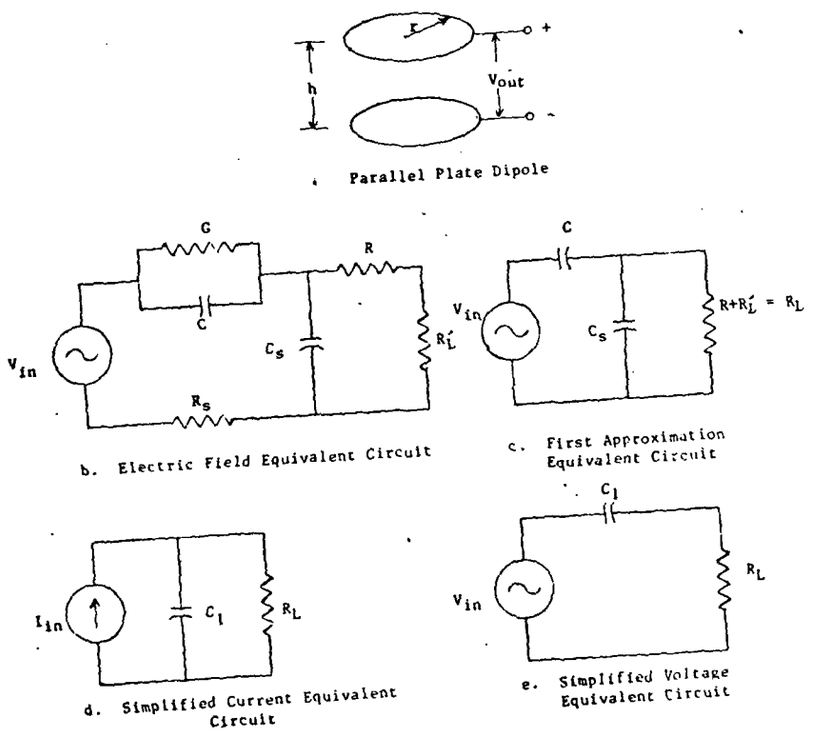

Figure 2 Electric Field Sensor and Equivalent Circuits

where K_E is the electric field sensor calibration constant. For A = 0.1 m^2 , $K_E = 4.425 \times 10^{-11}$ msec.

The sensor was calibrated using a 50 ohm parallel plane transmission line. A continuous wave test was performed using a sinusoidal excitation input with frequency range from 0.1 to 20 MHz. The theoretical value of K_E and the experimental value determined from the tests were within 10%.

Magnetic Field Sensor

The magnetic field sensor consisted of a turn one cylindrical moebius loop (Ref. 15) with a frequency response higher than 20 MHz. The sensor diameter was 0.0124 meter and the loop was constructed with semirigid coaxial cable to yield an equivalent area A of 0.02m^2. The sensors were installed with the bottom of the loop about 9 inches above the aircraft skin. Figure 3 shows the basic configuration. From Faraday's Law, it is known that a variation in the flux produces an induced voltage. Figures 3b and c show the sensor voltage and current equivalent circuits. R_s is the resistance in the turns of the wire, R_L is the load resistance, and L is the sensor inductance derived from Faraday's law. The effect of R_s can be neglected by choosing it much smaller than R_L. Since the input voltage is proportional to the derivative of the magnetic field density times the sensor area, the output voltage across R_L will be

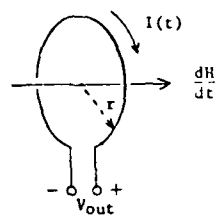

a. Inductive Loop

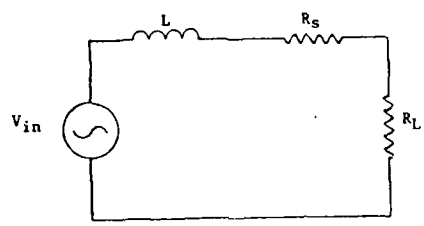

b. Simplified Voltage Equivalent Circuit

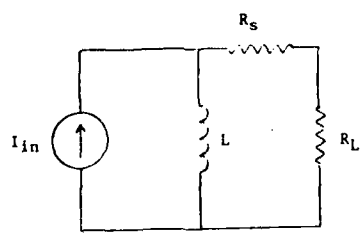

c. Simplified Current Equivalent Circuits

Figure 3 Magnetic Field Sensor and Equivalent Circuits

$$V_{out}(w) = jwB(w)\ A\ \frac{R_L}{R_L + jwL} \qquad (10)$$

For $w << \frac{R_L}{L}$, $V_{out}(w) = jwA\ B(w)$ (10a)

and the sensor voltage is proportional to the derivative of the magnetic field density. For $w >> \frac{R_L}{L}$, $V_{out}(w) = \frac{AR_L}{jwL} B(w)$ and the sensor voltage is proportional to the magnetic field. For the magnetic field sensors used, the measured value of L was 0.9H and R_L = 50 . Therefore, $\frac{R_L}{2\pi L}$ =8.85 MHz and the voltage reading was always proportional to the derivative of the magnetic field. In the time domain

$$V_{out}(t) = A_{eq}\frac{d}{dt}\ B(t) = K_B\ \frac{d}{dt}\ B(t) \qquad (12)$$

The value of K_B = A = .02 m^2 was verified with the parallel plate transmission line using the continuous wave test. The theoretical and experimental values agreed within 5%.

The low end frequency response of the magnetic field data channel was estimated in the same manner as was that of the electric field data channel. Using 0.6 and 0.01 A/m for the magnitudes of the magnetic field at 1 and 30 Km, respectively, the low end frequency response were estimated to be 20 KHz and 500 Hz, respectively.

Skin Current Sensor

The skin current sensors operate on the same principle as the magnetic field sensors. From Ampere's law it is known that

$$\int \bar{H} \cdot \overline{dl} = \int \bar{J}_s \cdot \overline{ds} + \frac{d}{dt} \int \bar{D} \cdot \overline{ds} \qquad (13)$$

But the magnetic flux incident on the sensor will be due

to the conduction current J because the induction term is negligible for no apertures. Applying boundary conditions for a conductor, H must be equal to J_S, so that:

$$\frac{B}{\mu_o} = J_S \qquad (14)$$

Using (12) and (14) the output voltage of the sensor can be expressed as:

$$V_{out} = A \mu_o \frac{dJs}{dt} \qquad (15)$$

Equation (15) is valid for good conductors with negligible skin depth over the frequency of interest (mainly between 0.1 and 20 MHz).

The skin current sensors consisted of the same type of loops used for magnetic field measurements except that the bottom of the loop was at the skin surface. The sensors were calibrated in the parallel plate transmission line using the same technique as for magnetic field sensors. A more extensive development of sensor theory can be found in Baum (Ref. 15).

Aircraft Configuration

Figure 4 shows the instrumentation used in 1981. The D-Dot FUF was integrated near the antenna and transmitter. This hardware integration was required to extend the low frequency response to near DC. The D output of the fiber optic receiver was stored in two FM channels with different gains. The frequency response of this channel was from DC to 500 KHz. The Q-Dot, B-Dot and the remaining D-Dot

sensor outputs were transmitted with fiber optic cables and recorded in two different forms. One output was left in derivative form, logged a ' could be stored in the digital transient recorder (DTR) and transferred to magnetic tape. The other output was integrated and could be recorded in analog form on direct record channels of the instrumentation recorded. The J-Dot sensor outputs were run through a logarithmic amplifier and transmitted with fiber optic cables to both the DTR and the magnetic tape recorder. Fuselage and wing wire transients were also connected to the magnetic tape recorder and the DTR.

Because of the noise level, the outputs from the fiber optic receiver for the latter signals could only be integrated down to 3 KHz. Only analog data was obtained for the two direct strikes presented in this thesis because the DTR triggered prior to the event.

Once the aircraft was instrumented as shown in figure 1, the electric and magnetic field sensors were calibrated. A rectangular pulse with known magnitude, risetime and falltime was incident at the parallel plate and the response at the recorder input was measured with an oscilloscope. This technique determined the value of K_E in equation (9) and the frequency response of the sensors.

The overall dynamic range of the integrated output from the electric and magnetic fields was designed for lightning flashes at distances from 0.5 KM to 30 KM. In

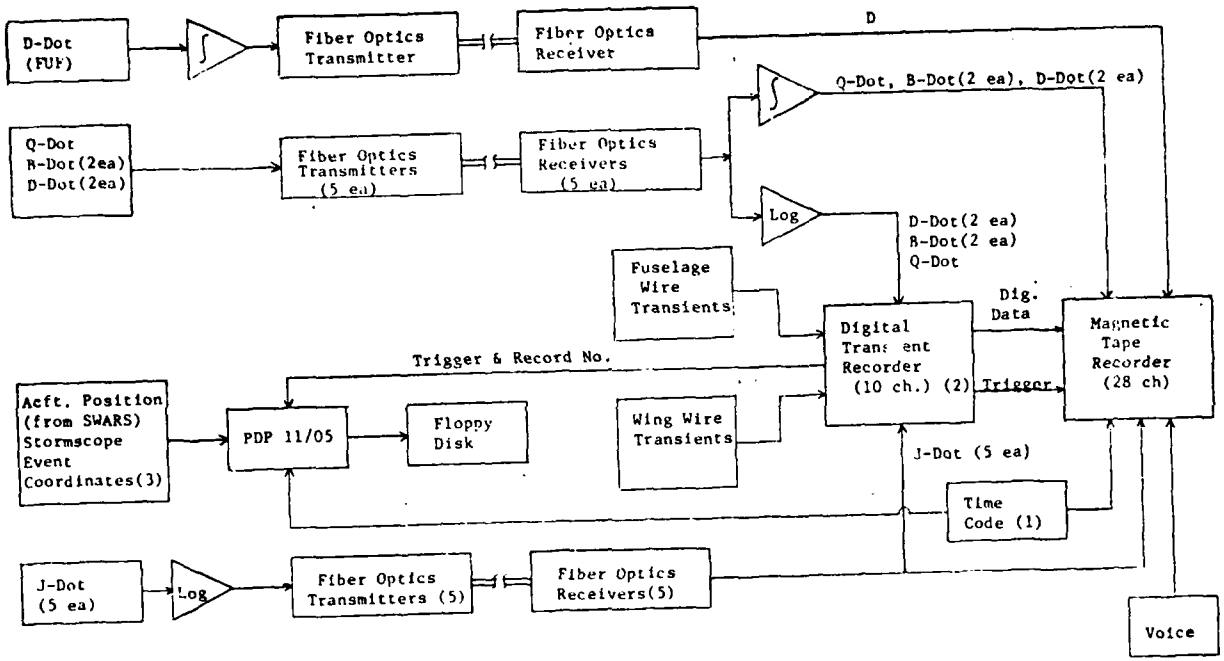

Notes: 1. IRIG B synchronized to WWV
2. Ten inputs, out of a possible twelve, selected before to each mission
3 On Stormscope evaluation missions only

Figure 4 FY91 Airborne Instrumentation Block Diagram

case o' the 26 Aug. direct strike, however, the output from the D-Dot sensor on the left wing tip was set for a maximum electric field of ??0,000 volts/meter and the $\dot{J}$ sensors were calibrated to measure skin currents on the order of tens of kiloamperes.

A Ryan Stormscope was mounted in the aircraft as part of a program to evaluate its performance and was used to assist in determining the relative locations of atmospheric electrical activity. It was located next to the aft lower fuselage next to the D-Dot sensor. With the exception of the stormscope display unit, all the aircraft instrumentation needed for operator interaction was located in one rack.

A periodic calibration with controlled output amplitude, frequency, and repetition rate was built and mounted in the aircraft. This calibration pulse was used to correlate the airborne and ground events.

Data Processing

The analog direct strike data acquired during flight was stored by a magnetic tape recorder with a 1.5 MHz frequency response as shown in the instrumentation block diagram. Figure 5 shows the technique used to transfer the analog data from magnetic tape to floppy discs. The data recorded in the Honeywell 101 was read into the Micro Pro recorder. The channels were stored on four displays and a trigger point was chosen by observing the

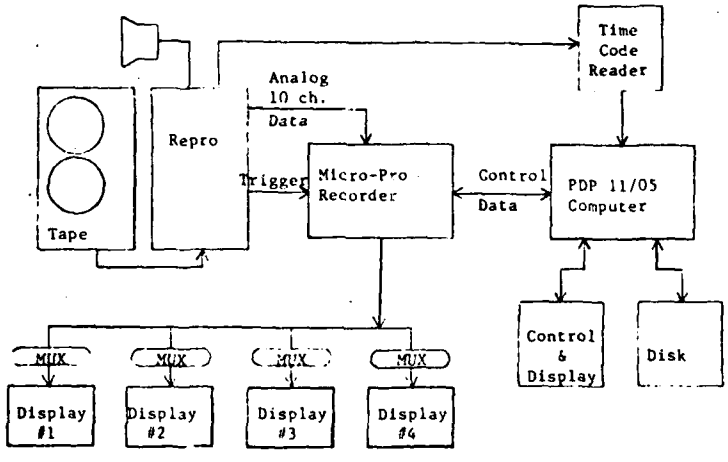

Analog Data Transfer

Figure 5 Techniques for Transferring Analog Data To Floppy Disc

analog data. Then the analog data was digitized by the Micropro recorder at various sampling rates. Each of these digital windows was transferred and stored on disc in the PDP 11/05 computer. For subsequent data identification, sweep rate, input range, trigger delay time, and the file and channel number of the data were also stored. Since the computer memory in the PDP 11/05 was limited to 10K, the data windows were read into the computer and stored on the disc as two 4096 data point arrays. A maximum of 10 channels could be processed with the same trigger due to the limited number of inputs to the Micro Pro.

Once the data was transferred to the PDP 11/05, several operations were performed to get the data into the form presented in this thesis.

The logged output data stored on floppy discs in the PDP 11/05 was first antilogged. The input and output valves to the log amp were first plotted and then a best fit curve obtained. From this plot the resulting antilog equation for the $\dot{B}$ and $\dot{Q}$ sensors was

$$V_{in} = \log^{-1} \frac{V_{out} - .6647}{.2163} \qquad (16)$$

and for the J and D sensors was

$$V_{in} = \log^{-1} \frac{V_{out} - .0888}{.0383} \qquad (17)$$

Before the data was antilogged the recorded output was scaled to the input range and the mean removed.

The detected voltage reading at the output of the sensor was integrated and properly scaled to determine corresponding readings of electric and magnetic fields. From Gauss's law, the current flowing in the cable connected to the electric field plate is given by

$$I(t) = \epsilon_o S \frac{dE(t)}{dt} \tag{18}$$

Since the voltage is measured across a 50 Ω load, equation (18) can be solved for the E field as

$$E(t) = \frac{1}{\epsilon_o S R} \tag{19}$$

The equivalent sensor area(S) was $.1m^2$ for Q-Dot and $.02m^2$ for D-Dot. Then substituting the values of ϵ_o, R, and S into equation (19), the integrated value of v(t) will be multiplied by 22598.9 and 112994 for Q-Dot and D-Dot, respectively. From Faraday's law, the detected voltage between the wires connected to the magnetic field sensor is

$$V(t) = \mu_o S \frac{dH(t)}{dt} \tag{20}$$

which can be solved for H as

$$H(t) = \frac{1}{\mu_o S} \tag{21}$$

By substituting the value of μ_o, an equivalent area(S) of $.02m^2$ for the $\dot{B}$ and $\dot{J}$ sensors, and time in microseconds, the integrated value of v(t) will have to be multiplied by 39.7887 to obtain the corresponding values of H(t).

The integration of the data windows was performed in the PDP 11/05 using the standard trapezoidal approximation.

That i ,

$$y(n) = y(n-1) + \frac{T}{2} x(n) \quad = x(n-1) \tag{22}$$

where y(n) is the output, x(n) is the input, and T is the time between samples.

The final processed data is referred to as follows. The integrated D-Dot FUF sensor output when multiplied by appropriate constants is referred to as E-FUF. The integrated Q-Dot is referred to as E AUF (aft upper fuselage). The other integrated D-Dot sensor outputs are referred to as E LWT (left wing tip) and E ALF (aft lower fuselage). The integrated B-Dot sensor outputs are referred to as H NT (Nose to tail) and H WW (Wing to wing). The J-Dot sensor outputs are referred to as $\dot{J}$ LLW (left lower wing), $\dot{J}$ LUW (left upper wing), $\dot{J}$ RLW (right lower wing), $\dot{J}$ RUW (right upper wing), and $\dot{J}$ AUF (aft upper fuselage). The integrated versions of these $\dot{J}$ sensor outputs remain in the same notation except without the dot over the J.

It should also be noted that the instrumentation was designed to measure near and far field data on lightning with simultaneous measurements being recorded at five ground stations. Therefore there is some additional instrumentation not mentioned herein that appears on some of the diagrams. For the two direct strikes reported on in this thesis, the aircraft was far away from the ground stations. It was not possible to correlate the

data from the ground and aircraft recorders. Rustan et. al. (Ref. 10) gave a more complete description of the entire instrumentation package.

Limitations

The aircraft instrumentation was designed such that only the E LWT (26 Aug.) and J Dot (both strikes) sensors would not saturate for direct strikes. All other sensors saturated during the strike because they were mainly designed for near and far field data.

Another limitation had to do with the low frequency response of the sensors. The E FUF sensor was calibrated to give a DC-500 KHz response for the 26 August flight. However as the aircraft became charged prior to the strike, this sensor drifted into saturation and remained saturated during the entire flash. Thus no low frequency response was measured. The remaining sensors had no frequency response below a few kilohertz and this factor must be kept on mind when analyzing the E field and H field waveforms. The widest pulse seen in any of these sensors is about 0.1 msec. This corresponds to 10 KHz which is the low frequency response of the sensors. The recorded pulses appear to be bipolar. However this is probably due to the drift experienced by the absence of low frequency response. The computer integration of J-Dot waveforms had to be interpreted carefully. All other sensor outputs were hardware integrated before they were recorded. However the J-Dot waveforms were integrated by the PDP 11/05 iteratively using equation (22), after the flights were completed. The computer integrated of the J-Dot waveforms

are not always consistent in all the data windows. The initial conditions of the integration routine is different for the various windows thus obtaining variation in the waveforms. An average risetime for the J-Dot waveforms was determined based on risetimes of random pulses over the entire flash. For the 26 August flash the value was 1 μsec and for the 17 July flash was 5 μsec. Then the $\dot{J}$ waveforms were estimated to increase and decrease linearly over this time to their maximum values. Thereby maximum J values could be estimated with about a 50% confidence factor.

The values for J and H in amps/meter were then converted to equivalent total current flow using calculations by Burroughs (Ref. 17). In his paper Burroughs tested the sensors at their respective locations to determine the value of J that would be read on the sensors given a total current of known magnitude applied to the nose of the aircraft. These calculations were done using a wire grid model of the airplane on a computer program. The results of the test are summarized in the following table.

Sensor Location	Conversion
J, H Fuselage	7.6×10^{-2} A/M per 1A
I, H Upper wing	7.3×10^{-2} A/M per 1A
J lower wing	7.4×10^{-2} A/M per 1A

Table VI Burroughs Conversion Factors

The values were then applied to the J and H readings and

the equivalent uniform currents were plotted to the right of all these plots on all the data windows.

Direct Strike 26 August

General

On August 26, 1981 at 17:09:45 EDT the aircrew reported a direct strike to the aircraft which was characterized by a loud noise and a small boom. The aircraft was flying at 333 KM/HR at an altitude of 16,000 feet. The outside air temperature was $+5^{o}C$. and the aircraft was flying inside a cloud in an area of slushy precipitation in a rapidly building phase of cloud formation. No lightning had been reported within 5 KM previous to this strike. There was a large anvil above the aircraft and cloud tops were estimated at 30,000 feet.

The conditions that the aircraft was flying in, are those summarized by Clifford (Ref. 13). The conditions that Clifford specifies as those most likely to be experienced during a direct strike are flying in a cloud in mixed precipitation at the freezing level at an altitude of 15-20,000 feet. The crew, which had extensive experience flying under adverse weather conditions, estimated that the attachment was made across the fuselage. However, even after intensive investigation, no pitting or burn marks could be found on the aircraft. This implies that the continuing current from this flash was either of very low magnitude or was nonexistent. The only sensor E FUF calibrated to give low frequency response to less than 1 Hz was saturated over the entire period of the strike

and th. instrumentation used for the rest of the sensors have a low frequency response of a few Kilohertz. Therefore, continuing current could not be measured.

The only damage incurred from the strike was two of the computer systems on board the aircraft. Memory dumps occurred to these two computers located in the forward fuselage behind the cockpit area. The power cables from these computers were located within a few inches of the internally monitored fuselage wire which recorded transients of only 40 mV.

Eight time windows were used to analyze this data; 800 msec, 400 msec, 82 msec, 4 msec, 1.6 msec, 164 μsec (2). For the most part the smaller windows are expansions of the next larger window. The exceptions to this will be noted when a new window is introduced. In addition several 164 μsec windows were plotted to determine the pulse characteristic with a resolution of tens of nanoseconds. Also peak currents using Burroughs (Ref. 17) calculations are plotted to the right of the applicable waveforms.

800 msec

The 800 msec window shows an overview of the entire flash (Fig. 8). The flash lasted 460 msec and can be divided into three phases.

The first phase lasted about 110 msec with the majority of the activity occurring in the first 30 msec. This portion of the flash is characterized by a large number

of discrete pulses with a decreasing pulse repetition rate and magnitude as time increases. The pulses start out so close together that it becomes difficult to fully recognize each pulse in all of the sensors.

The envelope of the pulses decrease in magnitude with time and appears to have an exponential decay with a time constant of about 6 msec. Peak magnitudes are discussed in the smaller time window sections to limit errors from undersampling.

The second phase of the flash is the quiet period after the first phase. This quiet period lasts about 240 msec during which time only a few low amplitude pulses were recorded on only the E ALF sensor.

The third phase of the flash occurs at about 0.4 seconds as shown in Figure (8). The fewer pulses in this phase are spaced further apart than in the initial phase with time between pulses ranging from 25 to 60 msec. Also the pulses are of varying amplitudes with the total duration of this phase lasting also about 110 msec.

The pulses of the third phase are well correlated on most of the sensors, especially the electric field sensors. There are at least five large pulses, although they are not correlated on all the sensors. The first pulse appears on all the electric and magnetic field sensors but not on the J or wing wire. For this pulse the magnitude of the electric field reaches $\pm$80,000 V/M on the

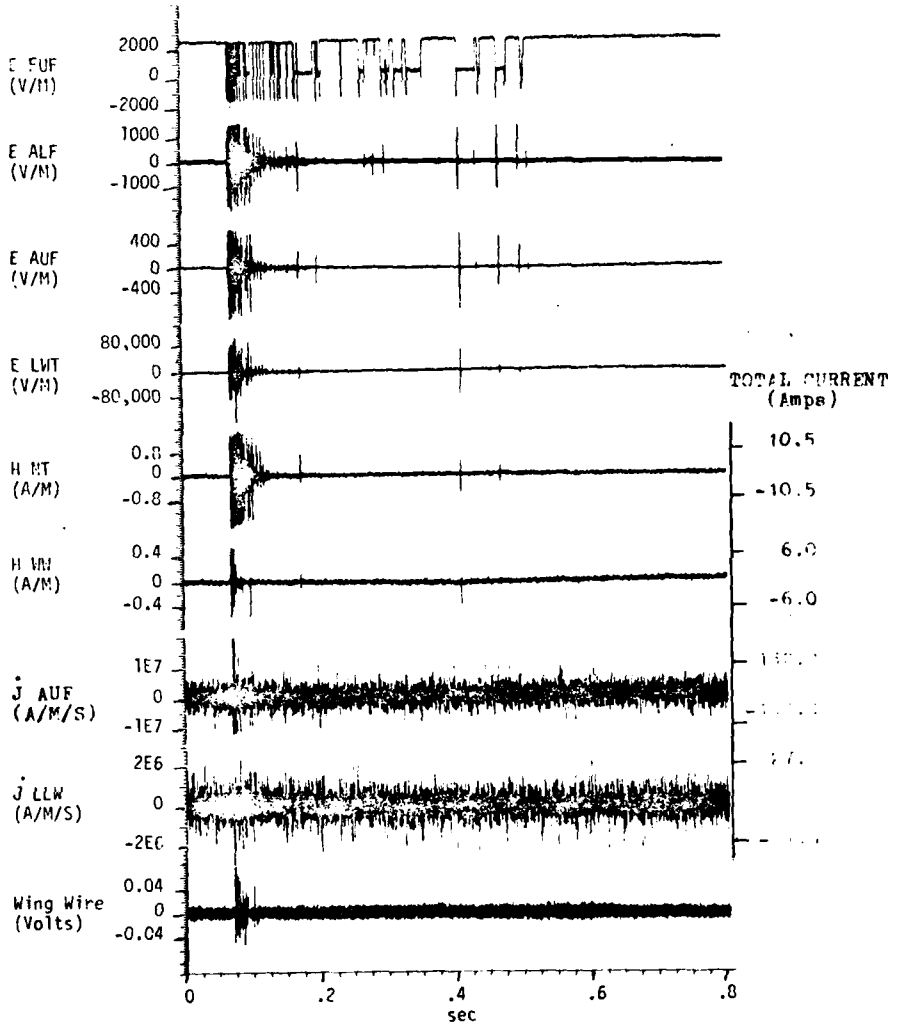

Figure 3 300 msec

E LWT. The other E field sensors are saturated at 800 V/M for E AUF and 2,000 V/M for E ALF. The H NT reading was .6 A/M and the H WW read .4 A/M. These represent the highest readings in the third phase of the flash. The remainder of the pulses are of lesser magnitude in all the unsaturated sensors. The time between pulses duration ranges from 25 to 60 msec which is well above the time between pulses that would be expected for either aircraft resonances (Ref. 8 and 10) or for dwell time between attachment points of less than 10 msec (Ref. 16). Even though the third phase lasts about the same duration as the first phase, it is much less active than the first phase. A time window of 164 msec is presented later to look at the fine structure of the first pulse of the second phase.

400 msec

The 400 msec window shows the activity in the first phase of the flash as well as most of the quiet period (Figure 9). The E field pulses during the active period of the first phase of the flash correlated well with H NT. The E and H sensors remain saturated for the first 20 msec of the flash with the exception of E LWT. The saturated portion of this active period is about 30 msec in all of these sensors. In the H WW however, saturation only occurred for some pulses in the first 20 msec and occurs primarily at the very beginning and end of this 20 msec

interval. Additionally, the J LLW sensor shows little correlation with the rest of the sensors. From the readings in all the sensors it is apparent that the predominant direction of current flow is directed along the fuselage and not across the wings. An interesting feature however on the internally monitored wires is that the voltage induced on the wing wire corresponds well with the amount of activity on the H WW record. But the current in the fuselage wire shows essentially no activity above the noise level during the entire flash. This is probably due to the placement of the wires in relation to the skin of the aircraft. The wing wire was placed along the inside portion of the wing just next to the skin. The fuselage wire however was centered along the fuselage remaining about a fuselage radius away from the skin except at one point where the wire was brought close to several windows to couple with the induced field due to aperture. The fuselage current flow in this area was probably low since most current flow was probably near the top or bottom of the fuselage and no significant current would flow around the windows.

The $\dot{J}$ sensors also show several interesting features. The $\dot{J}$ AUF sensor shows several large amplitude pulses at the beginning of the flash. These pulses seem to decay exponentially with time except for one rather large pulse some 30 msec after the start of the flash. The $\dot{J}$ LLW shows little activity above the noise level except for

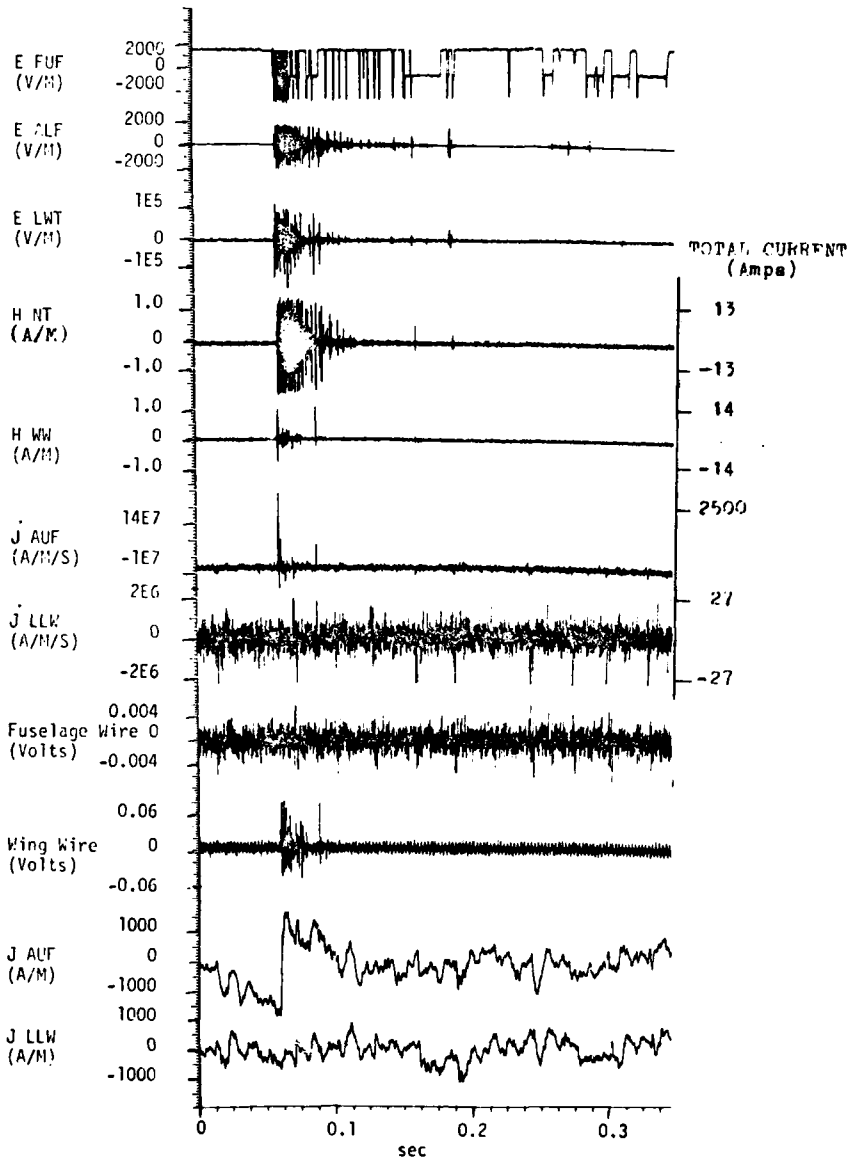

Figure 9 400 msec

several pulses some 12 msec after the start of the flash. There are also some discrete negative pulses of nominal amplitude spaced between 30 and 60 msec apart. These pulses do not correlate with the other sensors and may possibly represent some corona current off the wings.

82 msec

The 82 msec window (Figure 10) shows the first active portion of the flash in greater details. Clearly the J AUF activity is restricted to the first few milliseconds of the flash. This is because of the large magnitude of the current flow in the fuselage during this time (about 3 KA). The E ALF and H NT decrease in magnitude and repetition rate. The fuselage wire is clearly not affected by the activity in the E and H field sensors except for a single pulse at the very beginning of the flash.

A look at the wing wire shows that the first 20 msec of the flash was the most active period of induced transients on the wire. These transient pulses had magnitudes of about 50 mV. A total of about 30 pulses were induced on the wing wire during these 20 msec.

4 msec

The four millisecond window starts to show some of the finer details of the first few milliseconds of the flash. The first indication of the flash can be observed in the slow electric field change obtained in all four electric field sensors. Figure 11 shows four electric

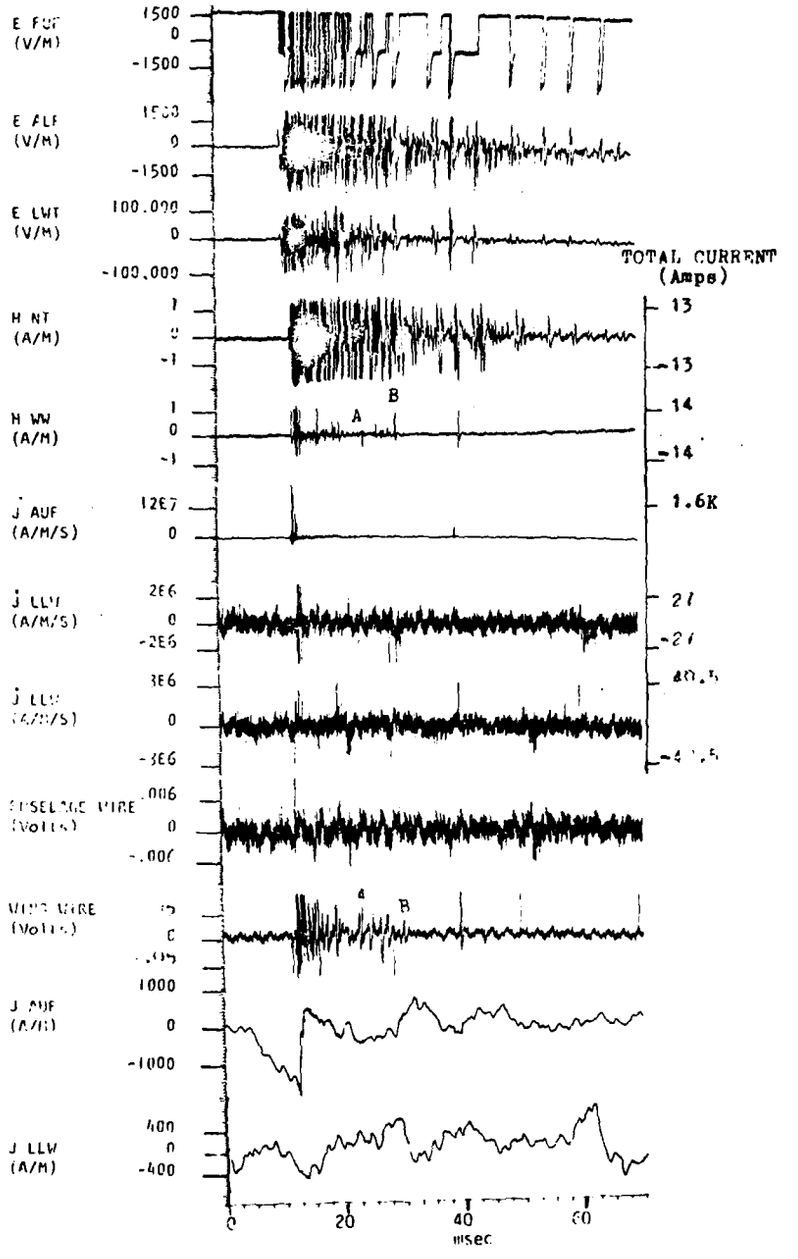

Figure 19 82 msec

field sensors, two magnetic field sensors, the $\dot{J}$ AUF and computer integrated $\dot{J}$ AUF sensor during the first 4 msec of the flash. The electric field change in the left wing tip first rises to 24,000 V/M over a 125 μsec period and starts to decrease slowly. About 350 μsec after the initial field change, the first fast field change occurs at the left wing tip. There were three fast field changes in the left wing tip in the order of few microseconds about 50 μsec apart. The first two pulses caused a field change of -24,000 V/M and the third was -60,000 V/M. The slow field change at the beginning of the discharge is an indication of a leader propagation; however, its short duration of 350 μsec before an abrupt discontinuity might indicate that pockets of charges were neutralized just a few hundred meters after the leader initiation. Also since no activity is seen in the H-field sensors during the slow electric field change, it can be assumed that the leader propagated from the cloud to the aircraft. If the leader had propagated from aircraft to cloud there should be some earlier evidence of current flow on the H field sensors that would be necessary to support leader propagation. Two points should be made about this observed leader. First leader propagation from cloud to aircraft doesn't necessarily mean a natural lightning flash. There is no other evidence of leader propagation past the aircraft, thus no natural cloud-to-ground or intra cloud

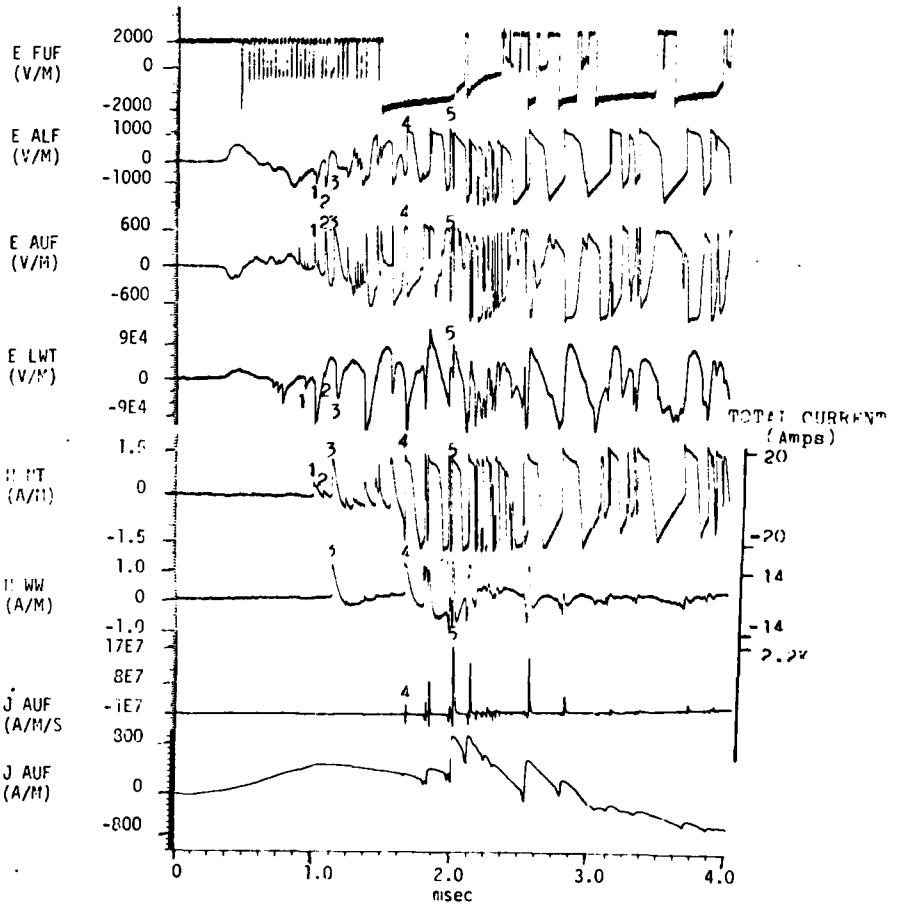

Figure 1' 4' msec

lightning takes place. Secondly, the length of the leader indicates that the charge center of the cloud and the aircraft are within 175 m of one another. Apparently the cloud charge center coming in contact via the leader with the aircraft does not produce a high enough field to propagate streamers between the aircraft and another charge center or the aircraft and ground. It seems reasonable to assume that this was a cloud-to-aircraft flash and not a natural lightning flash. The other electric field sensors during the initial 125 μsec period reached only -200 V/M in the aft upper fuselage and 1000 V/M at the aft lower fuselage with very small correlated fast field change for the first three sharp pulses which were observed in the left wing tip. This fact might indicate that field enhancement is larger in the aircraft wing tips. The first correlated fast field change in the first millisecond of the flash was observed about 680 μsec after the initial change. The field change at this time reached 100,000 V/M in the left wing tip, 400 V/M at the aft upper fuselage, and 900 V/M at the aft lower fuselage. This field change shown as pulse (1) in Figure 11 is the first magnetic field change detected and occurred in the magnetic field sensor oriented to read a maximum value for current flow along the fuselage. The magnitude of pulse (1) was 0.5 A/M and there was no correlated field change in the other transversal magnetic field sensor. Since the magnetic field sensor oriented to measure maximum for current flow

perpen icular to the fuselage was not located in the fuselage intersection with the wing but about three meters forward of the wing, it has less sensitivity to wing current than H NT sensitivity to fuselage current. The next fast field change shown as pulse (2) in Figure 11 is mainly observed in the fuselage electric field meter and in the magnetic field meter sensitive to fuselage current. Pulse (3) in Figure 11 is the first correlated pulse for both magnetic fields with readings of 1.4 A/M in the wing-to-wing direction and 1.3 A/M in the nose-to-tail direction. The actual magnitude of this pulse in the magnetic field sensors might have been larger than these values because these readings are near the saturation level. Pulse (3) correlates well with a pulse in the order of 600 V/M in the aft upper fuselage but the corresponding field change at the left wing tip and aft lower fuselage have a slower risetime. Pulse (4) in Figure 11 shows an interesting correlation. This is the first pulse which shows a correlated change in the J-Dot AUF sensor. The reading in the H NT sensor can be compared with the J-Dot AUF sensor. The J-Dot AUF sensor provides a reading for larger values of current flow along the fuselage which will saturate the H NT sensor. The reading in pulse (4) is equivalent to about 400 Amp current flow along the fuselage based on Burroughs model values. The reading in the AUF and ALF electric field sensors are saturated and the left wing

tip shows a correlated pulse of -150,000 V/M. This pulse occurred about 1.8 msec after the leader initiation. All the pulses in Figure 11 correlate quite well in all the sensors. Pulse (5) shows the largest current flow along the fuselage which corresponds to about 3,000 Amps flowing along the fuselage. The channel between the aircraft and cloud probably takes some time to become fully established after contact is made thus delaying the time before maximum current flow is seen. The time between the current bursts in the J-Dot AUF sensors ranges between tens of microseconds and several hundred microseconds. The four largest $\dot{J}$ AUF pulses, by using the average risetime technique and applying Burroughs model described earlier, corresponds to currents of 1.2 KA, 3.0 KA, 2 KA, and 2.2 KA respectively. They are separated from other pulses by 125 μsec, 80 μsec, 50 μsec, and 200 μsec. Given the shape of the current pulses, the charge on the aircraft for each isolated pulse discharge can be calculated. This was done for two of the pulses for the 164 μsec analysis and will be described later. The record of the $\dot{J}$ sensor in this flash corresponds fairly well with the French Transall (Ref. 5) classification of a type one flash. The French Transall data showed six flashes that fell into this catagory. One of the criteria for a flash of this type was four to eleven pulses. There were four major pulses in the 26 August flash. The maximum current for a type one seen by the Transall research was 4.5 KA. In this flash, the maxi-

mum wa 3 KA. The distance between the pulses was 8 to 200 μsec in the Transall data and the 26 August strike shows 50 to 200 μsec between pulses. The main differences in the French data were that they recorded a continuing current in each of their flashes.

There appears to be about 5-10 pulses per msec in the E field and H field sensors. If this can be considered an average value over the entire most active period of the flash (30 msec), then 150-300 pulses are characteristic of the most active period. Only about 10 to 20 additional pulses occur in the flash after the initial active period. It is important to note three features of the E and H field pulses. First, they are variable in duration. Some pulses are as short as several microseconds while others last up to 300 microseconds. Second is that about 1.1 msec after the start of the first fast field change, a 375 μsec period of rapid pulse repetitions occur. Since the start of this period coincides with the largest pulse on the J AUF sensor this 375 μsec period represents the majority of the energy transfer during the flash. There are about 14 pulses during this period in the E ALF, E AUF, E LWT, and H NT sensors. Finally no two sensors show a one to one correspondence in the relative magnitude of the waveforms for any of the pulses.

1.6 msec

The 1.6 msec window (Figure 12) starts after pulse

(3) on the 4 msec window which is about 1.25 msec after the beginning of the 4 msec window. The most interesting features on the 1.6 msec window relate to the pulses induced on the fuselage wire and the wing wire. The first pulse on the fuselage wire (A) registered about -5 mV and and correlated well with pulses in all other sensors. The E LWT recorded a value of -80,000 V/M. The H NT, E ALF, and E FUF saturated. A pulse of about 1.5 A/M was recorded on the H WW. The $\dot{J}$ AUF recorded a reading equivalent to about 500 A and the $\dot{J}$ LLW recorded about 400 A based on Burroughs values. The wing wire recorded a pulse that ranged from +100 mV to -50 mV. The second pulse on the fuselage wire (B) registered about +4 mV and correlates with the E LWT which recorded a pulse of -25,000 V/M. The H WW and $\dot{J}$ sensors also correlate well but show only slight magnitude discontinuities. The wing wire however showed the largest pulses varying from -120 mV to +140 mV. With a risetime of 10 μsec this corresponds to a $\frac{dV}{dt}$ of 2.6×10^4 V/S. This pulse shows the greatest voltage change seen in the wires during the flash. Seven other pulses in the fuselage wire were greater than 70 mV during the next 600 μsec with all of these pulses correlating well with the other sensors. The wing wire pulses correlate well with the $\dot{J}$ AUF and H WW sensors. The remaining E field and H field sensors may have shown similar correlation if they had not been saturated. However, by comparing

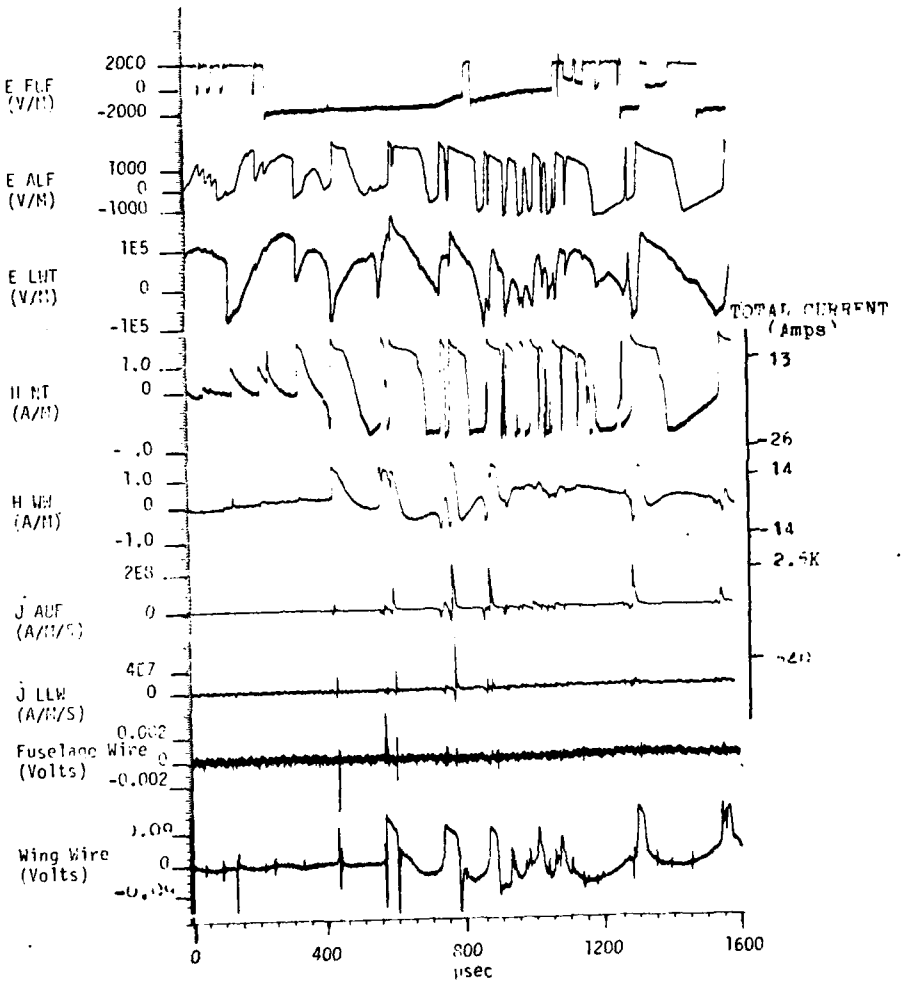

Figure 12 1.5 msec

the E and H of the non-saturated pulses an estimate of the maximum $\frac{dH}{dt}$ was obtained. Finding the maximum pulse in each of the non-saturated sensors indicate the following maximum estimated field changes.

Maximum

Current Change	$\frac{dI}{dt}$	3 KA/μS
E-Field	$\frac{dE}{dt}$	250,000 V/M/μS
H Field Change	$\frac{dH}{dt}$	3.2 A/M/μS
Induced voltage Change	$\frac{dV}{dt}$	26 KV/S

Table VII Maximum Changes

164 μsec

Two 164 μsec windows were plotted and correlated in this analysis. In addition, nine other 164 μsec windows were used to give an estimate of some of the pulse rise-times. These risetimes were calculated using the standard technique of taking the 10% to 90% of the fastest portion of the pulse. The two 164 μsec windows occur at the following locations: The first 164 μsec window is shown in Figure (13) and shows the largest current pulse of the flash. The second 164 μsec window occurs at the beginning of the second attachment and is shown in Figure (14).

The J integrations do not drift much on the 164 μsec windows so some comparisons are made to previous estimations.

Maximum J on the AUT sensor looks to be about 225 A/M. Using Burroughs (Ref. 16) calculations this yields an equivalent current of

$$(225)/(7.6 \times 10^{-2}) = 2.96 \text{ KA}$$

This agrees well with the estimated 3 KA from before using average risetimes. The other pulse has a maximum value of 200 A/M or an equivalent current of 2.7 KA, somewhat higher than the estimated 2 KA from before and was probably due to an underestimate of the risetime of the $\dot{J}$ waveform in the initial current derivation discussed earlier. There an average risetime of one microsecond was assumed. Actually the risetimes tend to increase with successive pulses.

Now integration of these two current pulses over time can be used to determine the charge transfer in each pulse. For a duration of the pulse about 20 μsec the charge by the transfer pulse is about 30 millicoulombs. These pulses probably account for most of the charge transfer during the flash. In a cloud-to-aircraft flash this aircraft charge is being neutralized by a charge of opposite polarity in the cloud. This probably occurs as a result of the channel finding pockets of charge within the cloud and then these charge pockets flowing down the channel and neutralizing the charge built up on the aircraft through triboelectric charging. Taking the pulse interval as 17.5 μsec and following a similar analysis for the second pulse we get a charge of 47 millicoulombs.

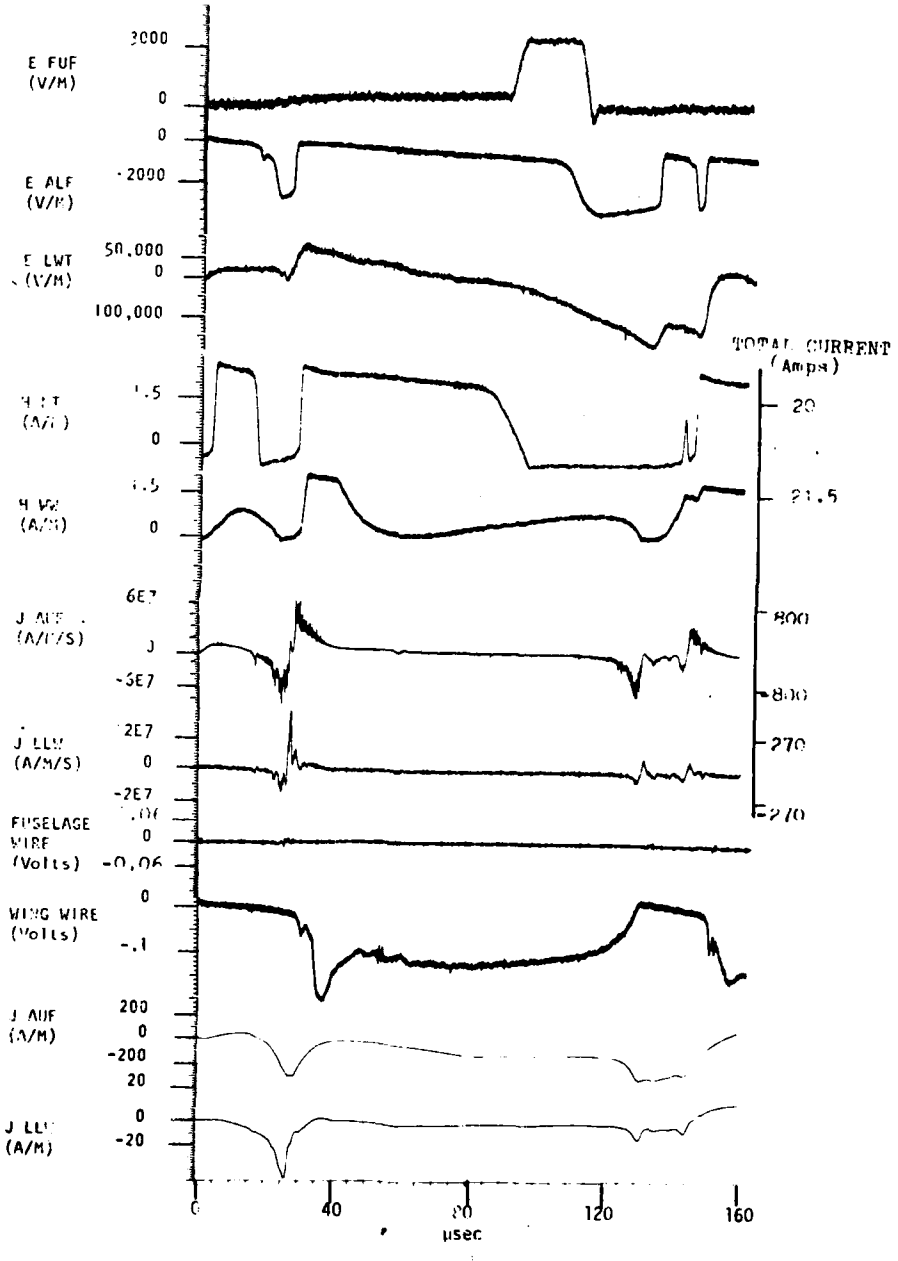

Figure 13 164 μsec

Since there was no sign of continuing current, these pulses seen on the $\dot{J}$ AUF sensor probably account for most of the charge transfer during the flash. The time between the end of the first current pulse and the start of the second pulse was analyzed to give some insight into the possible charging rate of the aircraft. First, a possible mechanism for what occurs during a charge transfer is postulated. Aircraft charge is neutralized by change in the cloud, then a period of recharging occurs until the next discharge occurs. Calculations by Shaeffer (Ref. 12) and Fisher and Plumer (Ref. 17) indicate that an aircraft can hold a charge from 0.1-3 mC of charge before corona starts to occur. These calculations may just be low Clifford (Ref. 13) has postulated that additional charging of the aircraft may occur if corona does not keep up with the triboelectric charging rate of the aircraft. This may explain not only the high charge on the aircraft but also the unipolar waveforms that are seen as the first fast field changes that occur before the first $\dot{J}$ pulse on the 4 msec window. If these changes are due to corona, then Clifford's posturlation would appear reasonable.

The last 164 μsec window that is analyzed in this section shows an expansion of the first pulse of the second attachment seen on the 800 msec window. The peak current levels during this attachment of only 150 A seen in the $\dot{J}$ AUF sensor is not as high as for the first attachment.

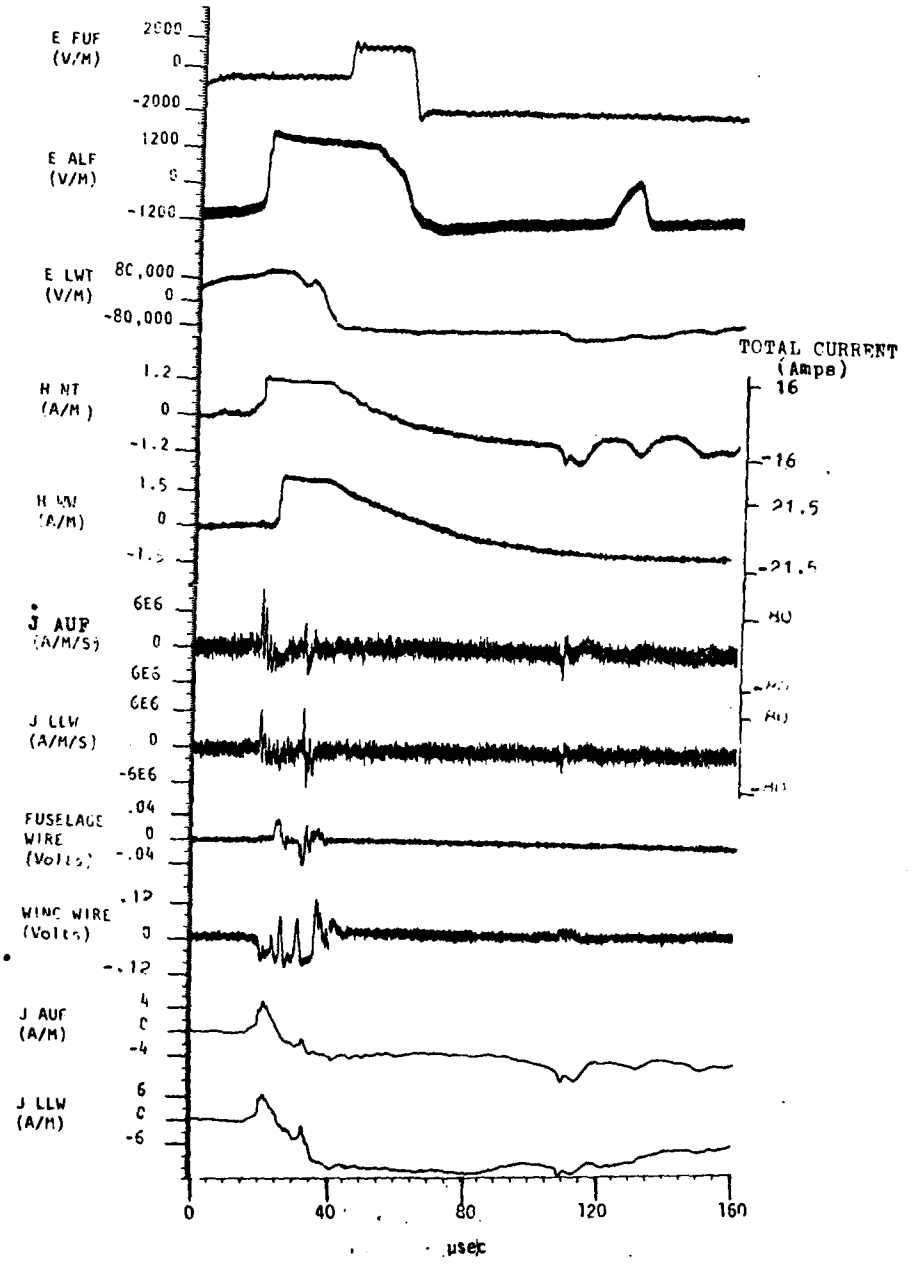

Figure 14 164 μsec

The E field and H field sensor magnitudes are also comparable with those of the first attachment. It is therefore deduced that the severity of the transients are not directly related to the magnitude of current flow on the surface of the aircraft.

Finally several other expansions were examined to determine risetimes. These results are presented in Figure (15). Risetimes were calculated using the standard 10% to 90% of the fastest portion of the curve. These risetimes represent only unsaturated pulses, so magnitude changes over the risetimes of the pulses are also presented. Maximum risetime seen was 3 μsec and minimum risetime was 248 nsec. The low risetime approaches the frequency limitations of the instrumentation. Figure 16 represents an expanded view of a pulse from the E LWT. Black lines drawn to indicate the points from which the risetime was calculated. Figure 17 represents an expanded view of a pulse from H WW again using the black lines as start-stop points.

Pulse #	1	2	3	4	5	6	7	8	9	
E LWT	2700	-	820	3000	2500	-	800	-	1100	Risetimes (nanoseconds)
H NT	1000	1468	400	-	420	1000	-	-	410	
J L	248	593	274	2003	800	-	800	331	2000	
J AUF	-	900	242	-	3000	-		410	-	
Wing Wire	-	1000	900	1500	2000	-	800	1000	2000	
Fuselage Wire	-	-	-	1500	310	1000	-	-	-	
E LWT V/M/μS	3.764	-	1.4E5	2E4	2.8E5	-	9.4E4	-	5.5E4	Magnitude Changes Over Risetimes
H NT A/M/μS	.05	.11	.75	-	1.66	.7	-	-	1.46	
J LLW A/M/μS	5.2	.51	.5	5.9	11.25	-	4.6	5.43	11.5	
J AUF A/M/μS	-	1.0	1.65	-	6.33	-	-	4.39	-	
Wing Wire V/μS	-	.019	.13	.166	.07	-	.175	.22	.12	
Fuselage Wire V/μS	-	-	-	.002	.13	.03	-	-	-	

Figure 15 Risetimes for 26 August

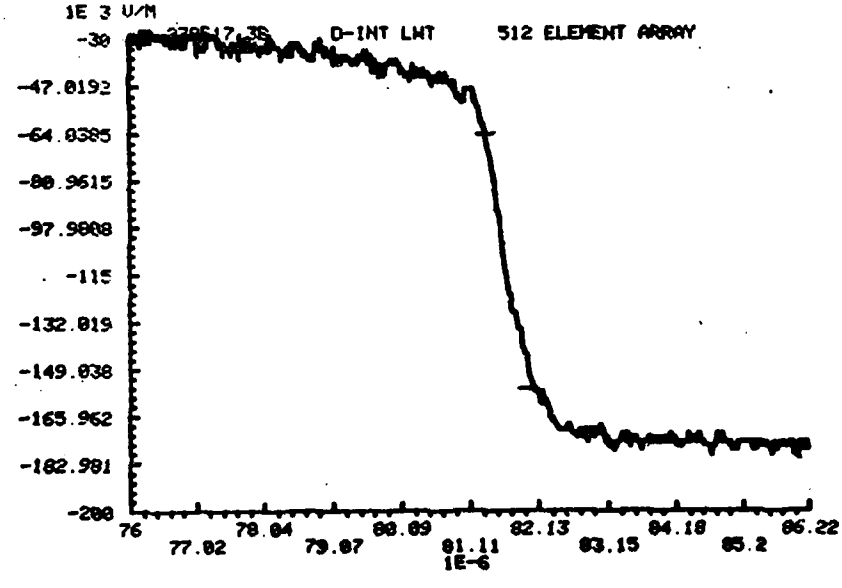

Figure 13 Expanded E LNT WaveForm for Risetime Calculation

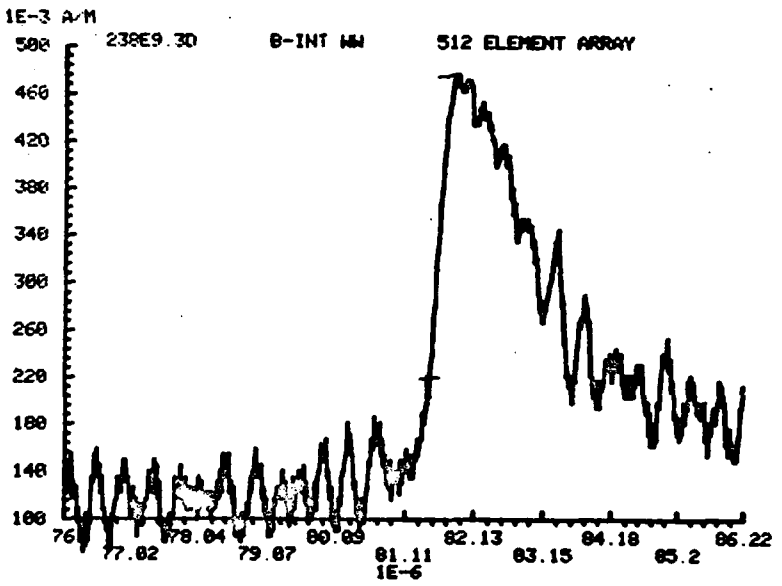

Figure 17 Expanded H WW waveform for risetime calculation

17 July 1981

On July 17, 1981 at 17:21:44 EDT the aircraft experienced a direct lightning strike. The aircraft was flying at 405 KM/HR at an altitude of 17,046 feet inside a cloud. The outside air temperature was -0.7°C and light rain was falling. The aircraft was experiencing light turbulence and the nearest thunderstorms were about 2 to 3 miles away. The cloud was estimated to be in the developing growth phase with maximum tops at 22,000 feet. No anvil was sighted above flight level. The approximate position of the aircraft was plotted on the National Weather Service radar picture from Miami five minutes before and one minute after the flash as shown in Figures 18 and 19. The contours shown in continuous lines represent regions of precipation or clutter as detected from the Miami ground radar. The dash lines encircle regions of high precipitation as detected from the aircraft radar. Finally, the crosses indicate location where the stormscope on board of the aircraft had detected lightning flashes.

Damage to the aircraft was done by the swept stroke of the continuing current in nine fastening screws along the upper fuselage at various points. Also the aircraft antenna wire mounted between the upper fuselage and the stabilizer was burned in half.

The instrumentation for this strike was similar to

the 26 August strike with several exveptions. The E LWT was calibrated to only measure a maximum value of 2000 V/M and there were no fuselage or wing wires in the interior of the aircraft.

Six time windows were assembled for this strike (400 msec, 82 msec, 4 msec (2), 1.6 msec and 164 μsec). The sensor outputs presented here are E FUF, E ALF, H NT, H WW, $\dot{J}$ AUF, $\dot{J}$ LUW, $\dot{J}$ LLW, $\dot{J}$ RUW. Integrated $\dot{J}$ sensor outputs are shown only at 164 μsec. Current values based on Burroughs calibration constants are plotted to the right of the plots. For $\dot{J}$ plots, an average risetime of 5 μsec with a linearly charged J is assumed.

400 msec

The 400 msec window in figure 20 shows that the entire flash lasted about 295 msec which can be classified in two intervals. The first interval is very active and lasted about 80 msec. This 80 msec active interval consisted of two distinct periods. The beginning of the flash had a high pulse repetition rate of 10 pulses per millisecond for about 43 msec and the following 25 msec had a slower pulse repetition rate of about 2 pulses per millisecond. The remaining period of the flash contains mainly discrete pulses of varying amplitudes separated in time from 6 to 75 msec. All of the sensors saturated at the beginning of the flash with exception of the H WW and the $\dot{J}$ sensors.

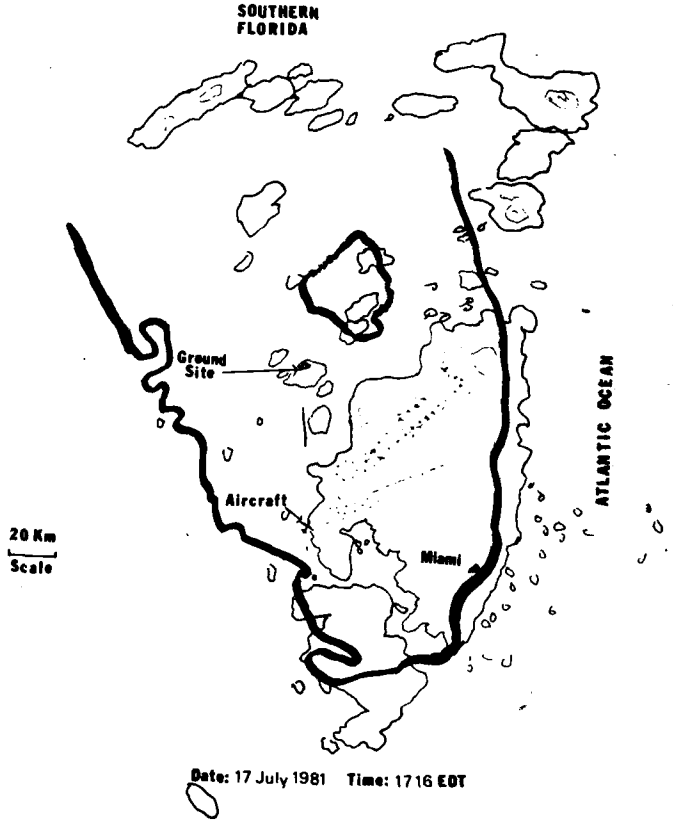

Figure 18 NWS Radar Miami

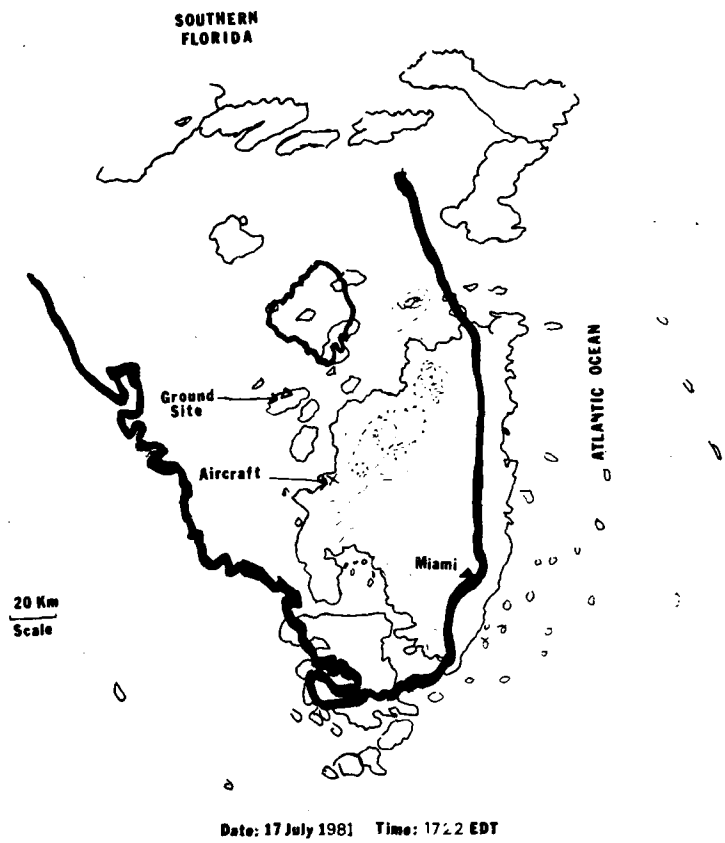

Figure 19 NWS Radar Miami

The maximum value observed on H WW was about 1.0 A/M which corresponds to a current of 14.3 A according to Burroughs (Ref. 16). The maximum value seen on the $\dot{J}$ sensor corresponds to about 650 A.

There are several interesting differences between this strike and the 26 August strike that can be seen on the 400 msec window. First in this strike the two phases of the flash are not as easily divided as in the 26 August flash. The 17 July flash might have had only one attachment while the 26 August flash might have had two. It seems to correlate well with the fact that on 17 July, the flash lasted a total of 295 msec while the 26 August flash lasted a total of 460 msec which is over 1½ times as long. In addition the entire flash is of less intensity for 17 July than for 26 August. Also the most intense portion of the 26 Aug. flash lasted several milliseconds longer than the 17 July flash. The highest reading for the $\dot{J}$ AUF sensor for the 17 July flash appears to occur at several different times over the first 20 msec of the flash with peak current values on the order of 650 A. This is in sharp contrast to the 26 August strike where the peak current values of several kiloamps occured after 1.3 msec of the first fast field change of the flash.

Another difference between the two flashes is the period immediately following the initial most active phase. On the 17 July flash there is a 25 msec period of intense

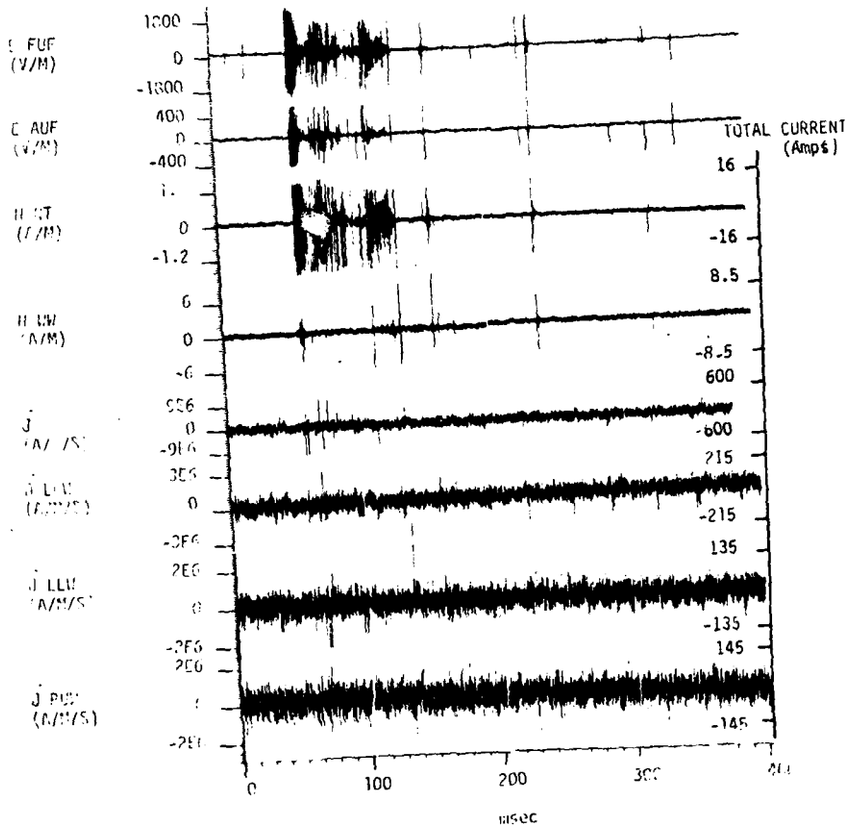

Figure 27 400 msec

activity on the E FUF, E AUF, H NT AND H WW. However, the 26 August flash shows little significant activity after the initial active period other than isolated pulses until the second attachment.

There are also several similarities between the two flashes that can be seen in the 400 msec window. The most active period in the E and H field sensors occurred during the initial 30-40 msec of the flash. Both flashes also exhibit discrete pulses. The pulses tend to be greatest just after attachment and decrease exponentially for the most active period. For the 17 July flash the time constant of the decay is about 8 msec. This is somewhat higher than the time constant of 6 msec seen in the 26 August flash.

82 msec

The 82 msec window in figure 21 shows several important features. First, the train of pulses that occur in the initial active period on the E field sensors start to decrease in magnitude for several milliseconds after the first 10-15 msec then increase again for 10-15 msec.

The 17 July strike showed evidence of a swept strike. This implies a continuing current, however during this flight none of the aircraft sensors were calibrated to pick up a DC current reading. Therefore a laboratory test was done in an attempt to determine the current necessary to produce the same amount of damage as was seen on the aircraft.

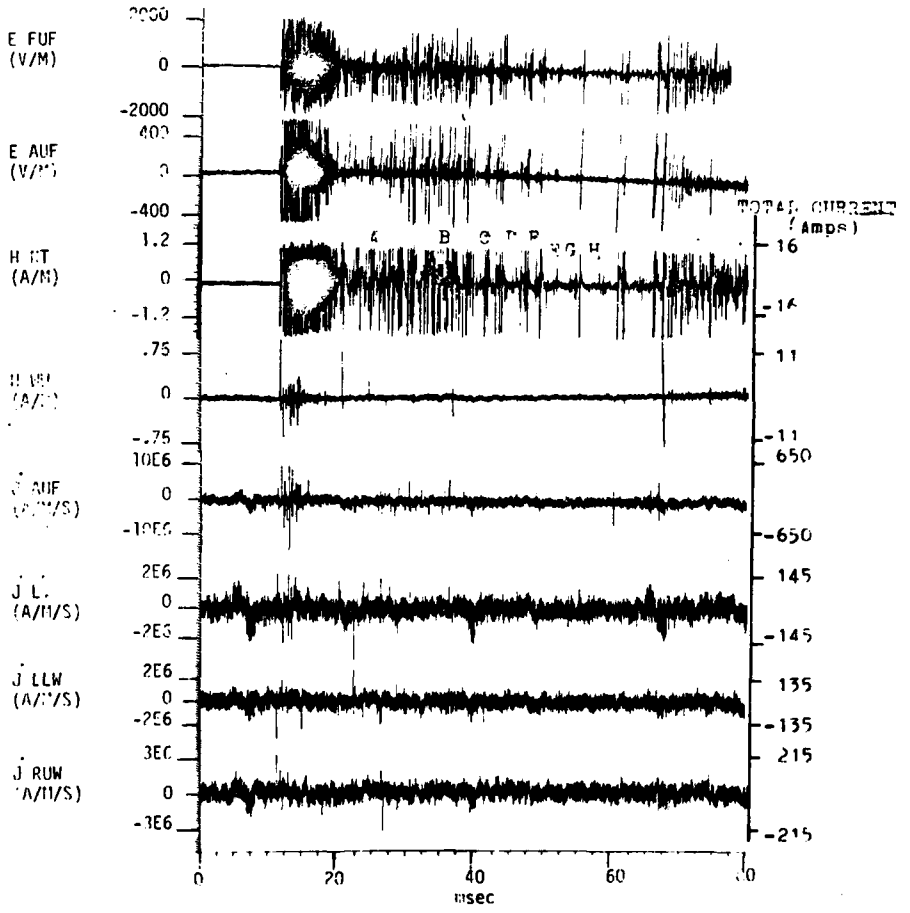

Figure 21 32 msec

The swept strike produced burns on nine screws along the fuselage. The following table shows the distance between points of attachment

	CM	dwell time (msec)
A 1-2	158.8	14.1
B 2-3	121.9	10.8
C 3-4	69.9	6.2
D 4-5	50.8	4.5
E 5-6	34.3	3.0
F 6-7	34.3	3.0
G 7-8	33.7	2.9
H 8-9	35.6	3.3
		47.7

Total distance between points 1 and 9 = 212.25 inches = 5.391 meters.

Table VIII Dwell Times

The aircraft was flying at 405 Km/Hr or 112.6 m/sec. The distance the total attachment swept can be assumed to be the distance between points 1 and 9 of 5.391 meters. The total duration of the swept strike can be determined from Plumer as (Ref. 17) $D=vt$ or $\frac{D}{v} = t$

5.39m/112.6m/s = .047 sec = 47 ms for total attachment

It is not known how long the strike dwelled on the ninth screw since no distance to next screw can be measured. The average dwell time is

$$\frac{\text{Total dwell time}}{\text{number of dwells}} = \frac{47.7 \text{ msec}}{8} = 5.96 \text{ msec/dwell}$$

This is about 1 sec longer than the value presented by Plumer (Ref. 17 p. 146) of 4.8 msec for dwell time on a painted surface with an airspeed of 112 m/sec.

Two important features on the dwell times can be seen. First the dwell times or distance arc travels decrease with time as the strike moves down the fuselage of the aircraft. It would seem that the strike would move equal distances in each case or at random. Secondly, the amount of damage to the screws was not a function of dwell time. The most damage was done to screws 4 and 5 which had some of the lowest dwell times. This implies that the charge transfer must be greatest in the central portion of the continuing current.

The sensor which is most likely to pick up the discontinuity of the current jumping from one dwell point to the next is the H NT sensor. This sensor is sensitive to current flow along the fuselage. The 82 msec window was examined for possibly pulses corresponding to the point to point jumping of the continuing current. The letters A through H over the H WW plot (Fig. 21) represent a possible time span for the swept strike. Furthermore at points where these pulses can be identified as single discrete pulses (points A, D, F, H), these pulses are positive going only - which is not characteristic of most of the pulses in the flash.

Next a determination of the continuing current was made by laboratory testing as shown in figure 22. Dif-

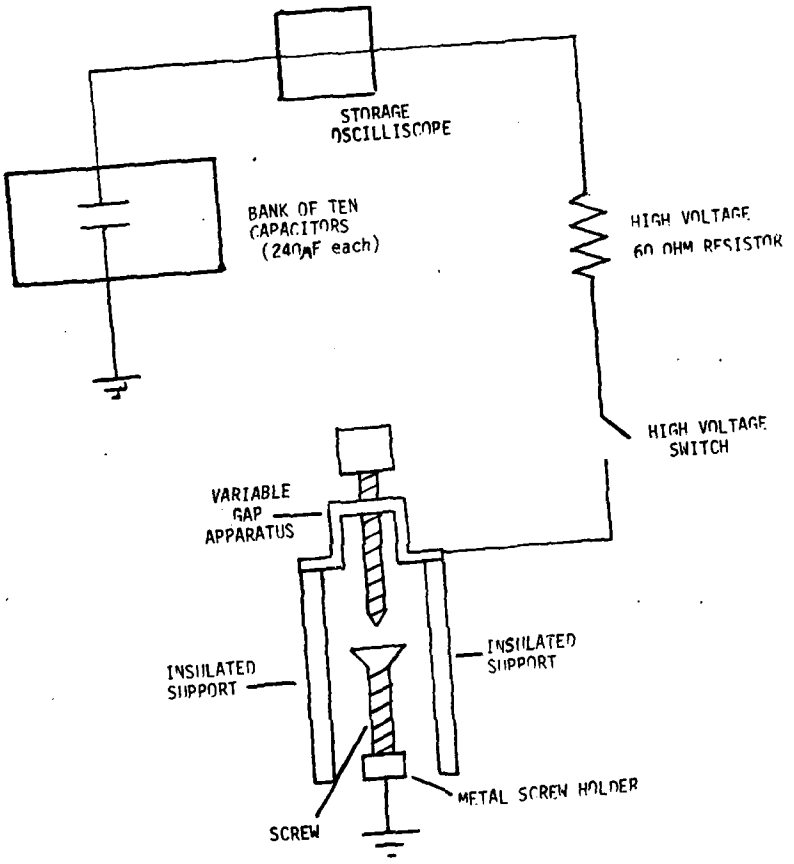

Figure 22 Test Configuration

ferent current values were applied to a screw in the following fashion. Ten 240 μF capacitors were connected in parallel for a total capacitance of 2.4 mF. They were connected in series to a 60 Ω resistor. Also in the circuit there was a device which held an aircraft screw and created a variable air gap over the screw as shown in figure 21.

The time constant of the circuit was

$$RC = (2.4 \times 10^{-3})(60) = 144 \times 10^{-3} \text{Sec} = 144 \text{ msec}$$

A current meter measured the current in the circuit and displayed the results on a storage oscilliscope. The capacitors were charged to 3 KV and the switch was closed creating an arc in the air gap. The oscilliscope recorded an initial current of 40 A that decayed to 30 A in 9 msec. After 9 msec the arc stopped when the voltage across the gap fell to less than the breakdown voltage. Damage to the screw was examined by two of the personnel that witnessed the actual damage to the aircraft to obtain an average damage amount with that done to the nine aircraft screws.

Therefore the estimate of charge transferred in the continuing current is

Taking the value of 9.0 ms for T_o and the average I of 35 A we get $\frac{40 + 30}{2} = 35$ A

If the charge transfer per dwell time of 5.96 msec for the actual flash is assumed to be .315 coulombs then the continuing current can be estimated as

$$I = \frac{.315 \text{ coulombs}}{5.96 \text{ msec}}$$

$$= 52.9 \text{ A}$$

Finally the amplitude of the pulses that corresponded to the dwell times was estimated from the H NT plot (fig. 21). The average value was about .6 A/M. Using Burroughs (Ref. 16) calibration constant of

$$7.6 \times 10^{-2} \text{ A/M per amp of current}$$

This corresponds to a current change of

$$(.6\text{A/M}) \left(\frac{1 \text{ amp}}{7.6 \times 10^{-2}\text{A/M}}\right) = 7.9 \text{ amps of uniform current flowing along the fuselage}$$

This value is about 6 times lower than the estimated value which probably means that the path of the current was not distributed uniformly in the fuselage cross section but most current flow was in a narrow strip on the top of the fuselage.

It should also be noted that the main activity (as far as current flow is concerned) is in the H NT sensor and the J AUF sensor thus suggesting an attachment along the fuselage. This correlates well with the path of the observed continuing current burn marks.

A final feature of the 82 msec window is the correlation between the H WW and J AUF sensors. The highest

amplitude group of pulses for both sensors was restricted to the first 5 sec of the flash and could also be seen on the other E and H field sensors had they not been saturated.

4 msec

The two four millisecond windows shown in figures (23) and (24) cover the first 8 msec of the flash. The first 4 msec window begins with the activity just prior to the start of the flash and the second 4 msec window begins about the time the first 4 msec window ends (see fig.21).

The first 4 msec window (fig. 23) shows the first evidence of the flash. A show field change of about -1800 V/M occurs in the E FUF sensor during a period of about 42 μsec. Also during this period the E AUF sensor increases to about 200 V/M. Again these low frequency pulses suggest a leader propagation. Since the E FUF recorded a greater field change it can be assumed that the leader was closest to the nose and extended to higher altitude. Also there is some activity in the H NT sensor during this period, indicating direct flow along the fuselage. This may indicate that the leader is propagating from the aircraft to the cloud charge center or possibly a streamer leaving the aircraft to meet the leader propagating down from the cloud.

The first fast field charge of the sensors occurred about 190 μsec later and is seen on the E FUF which recorded

a pulse from -900 V/M to 2400 V/M. Also the E AUF and H NT record correlated pulses from +600 V/M to -400 V/M on the E AUF and +1.5 A/M to -1.75 A/M on the H NT. The second correlated pulse was represented by a reading on all of the sensors and was the first fast field change seen on the H WW and all of the $\dot{J}$ AUF sensors. This was one of the highest amplitude pulses on the H WW of about .7 A/M. The $\dot{J}$ AUF sensor measured a value corresponding to a current of about 300 A while the $\dot{J}$ LUW, $\dot{J}$ LLW and $\dot{J}$ RUW measured about 250 A, 100 A and 150 A respectively. Since the current flow in the LUW is greater than the LLW, the lightning channel probably first attached to the upper part of the aircraft.

The remainder of the $\dot{J}$ sensor readings seem to correlate well with one another and with the $\dot{J}$ AUF recording four pulses over 500 amps and one pulse near 800 amps. Several differences are evident in the $\dot{J}$ AUF sensors for the 26 August flash and the 17 July flash. The 26 August flash had four pulses in the kiloamp range and were spaced 50-200 μsec apart. For the 17 July flash there are at least 10 pulses greater than 300 A and these occur at intervals from 50 to 400 μsec apart. This 17 July flash could correspond to the arbitrary type 1 flash as proposed by the French (Ref. 5) as in the 26 August flash. However the correlation is somewhat less since 400 μsec separation time exceeds the French criteria of 200 μsec. The con-

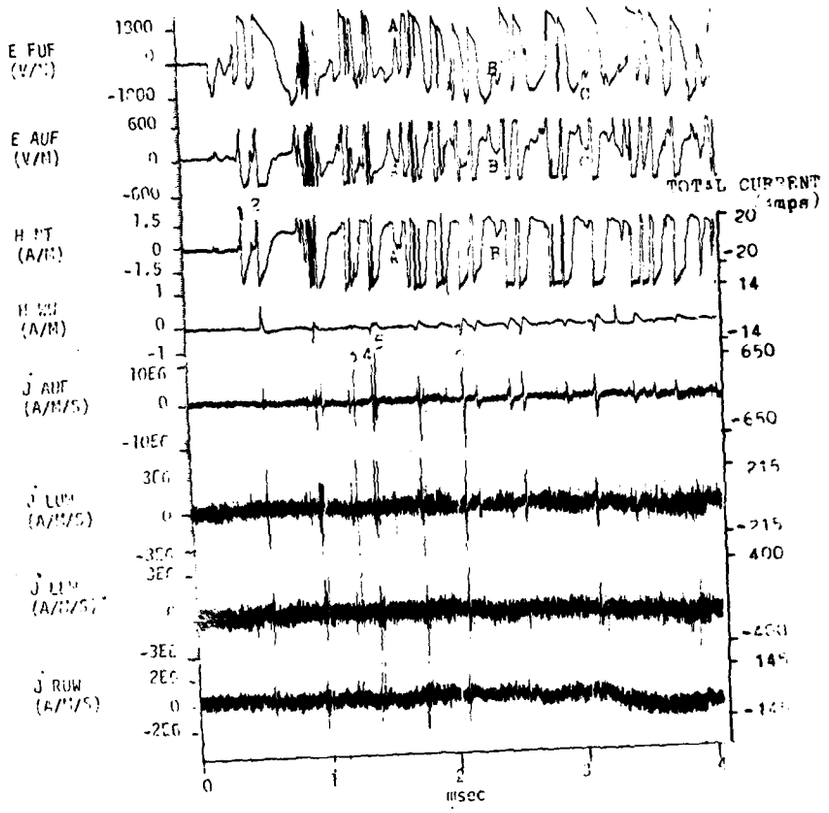

Figure 23 First 4 msec

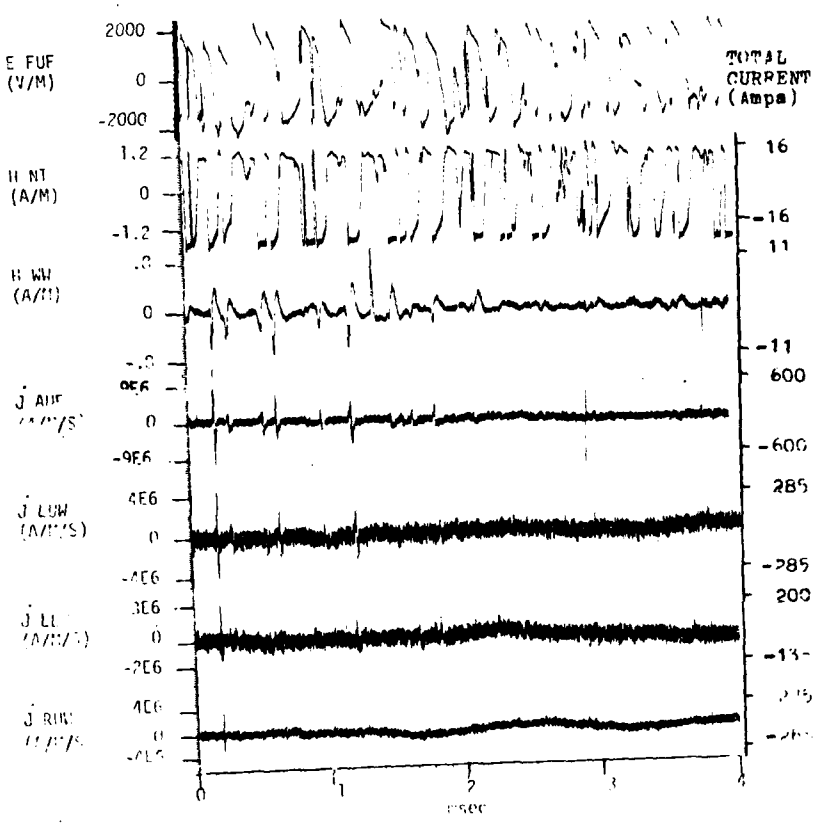

Figure 24 Second 4 msec

AD-A118 075 AIR FORCE INST OF TECH WRIGHT-PATTERSON AFB OH SCHOO--ETC F/G 1/2
DIRECT LIGHTNING STRIKES TO AIRCRAFT.(U)
JUN 82 J S SCHOWALTER
UNCLASSIFIED AFIT/GE/EE/82J-12 NL

tinuing current also is less for the 17 July flash since the French recorded continuing currents on the order of kiloamps while we experienced only 50 A.

The first 4 msec window shows a fast train of pulses in the E FUF, E AUF, AND H NT sensors about 600 μsec after the first fast field change (pulse 1). This pulse train lasts for about 125 μsec. Recall that the 26 August flash showed a similar pulse train with a higher pulse repetition rate. However on the 26 August this period occurred 1.1 sec after the start of the first field charge and lasted for about 375 μsec. These pulses also correlated with the highest current pulse recorded. The 17 July flash did not show this correlation but the total number of pulses (between 10 and 15) appears to be the same as in the 26 August case.

The second 4 msec window shown in figure 24 has several features that cannot be seen in the first 4 msec window. The H WW sensor shows little activity after 2.1 msec. The LUW sensor pulse repetition rate is higher than the RUW sensor indicating non-symmetrical current flow. There is a large current pulse on the J AUF which is expanded on the 164 μsec window and will be discussed there.

There are several features that can be seen when looking at both 4 msec windows together. First the total number of pulses can be estimated. There are around 70 discrete pulses during the 7.5 msec after the initial fast

field change or a little less than 10 pulses per millisecond. This result agrees with the pulse repetition rate calculated on this size window on the 26 August. However, these pulses do not occur in a repetition basis which could suggest that they are related to any of the aircraft resonant frequencies.

The total number of pulses for the flash was estimated at between 180 and 200 pulses by looking at the 82 msec and the 400 msec windows shown in figure 20 and figure 21.

A final observation of the 4 msec windows is on the nature of the pulses recorded on the E FUF, E AUF, and H NT. There are small slow field change pulses that are superimposed on the fast field change waveforms. They seem to correlate well with one another. (Letters A-C figure 23). These pulses are of equal or lesser amplitude as the stepped leader with the same general shape as the leader pulse. Also the polarity of these pulses is opposite that of the stepped leader in all three sensors and the pulses occur at an average of every 1 msec. These pulses are probably due to streamering of the aircraft fuselage.

1.6 msec

The 1.6 msec window shown in figure 24 is an expansion of a portion of the second 4 msec window. Some of the slow field change pulses are also seen on this

window and again show good correlation in the E FUF, E AUF and H NT sensors.

164 μsec

The 164 μsec window is shown in figure 26 and is an expansion of the section shown in figure (24) on the 1.6 msec window. This is the only window that uses the computer integration routine of the $\dot{J}$ sensors. Calculations of charge transfer were done in a similar method as for the 26 August flash. A notable feature of the $\dot{J}$ and J waveforms is the relatively slow risetime of the waveform. Using a triangular approximation of the J AUF waveform a peak value of 60 A/M will correspond to a current of

$$I = (60A/M) \cdot 1A/7.3 \times 10^{-2} A/M = 815A$$

or a charge of

$$Q = (815)\ (10^{-5}) = 8.15 \times 10^{-3}\ C = 8.15 \text{ millicoulombs}$$

This is a factor of 4 to 5 times less than was transferred per pulse on the 26 August. It is however slightly larger than the value of several millicoulombs suggested by Shaeffer as the maximum charge an aircraft can hold. It should also be noted that the 815A reading is somewhat higher than the 650 A value calculated in the approximate scale of current values. The risetime of this particular waveform was somewhat higher than the average value of 5 μs used in the calculation.

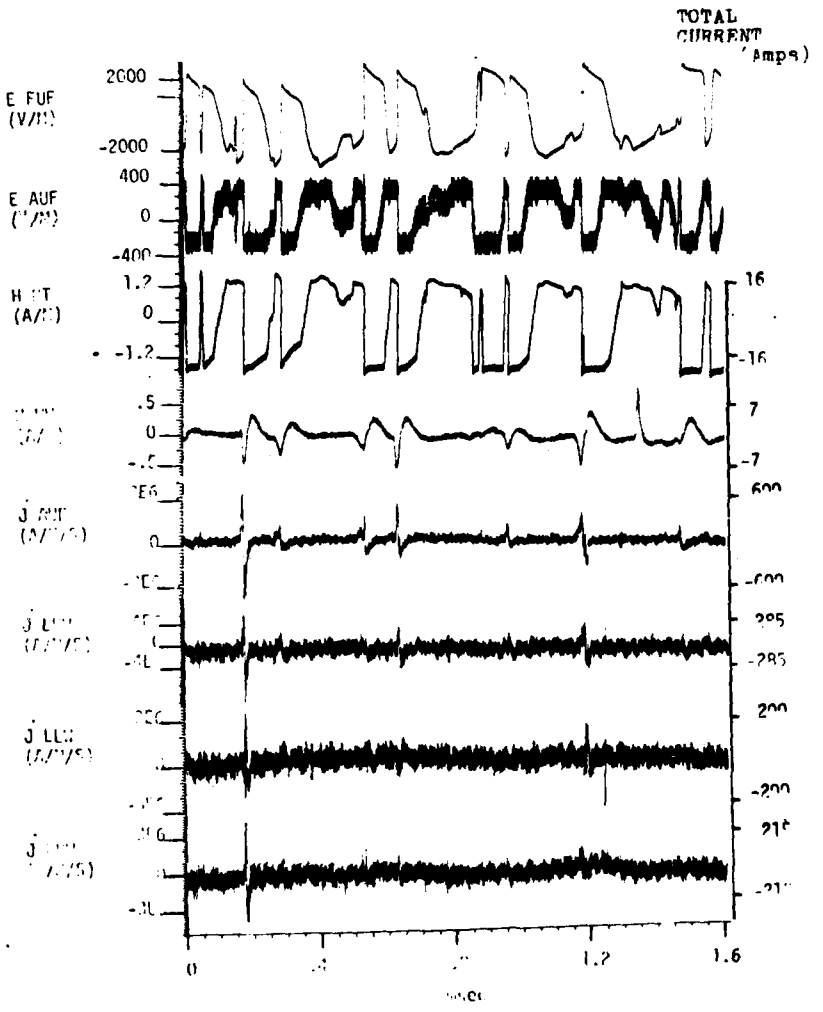

Figure 25 1.6 msec

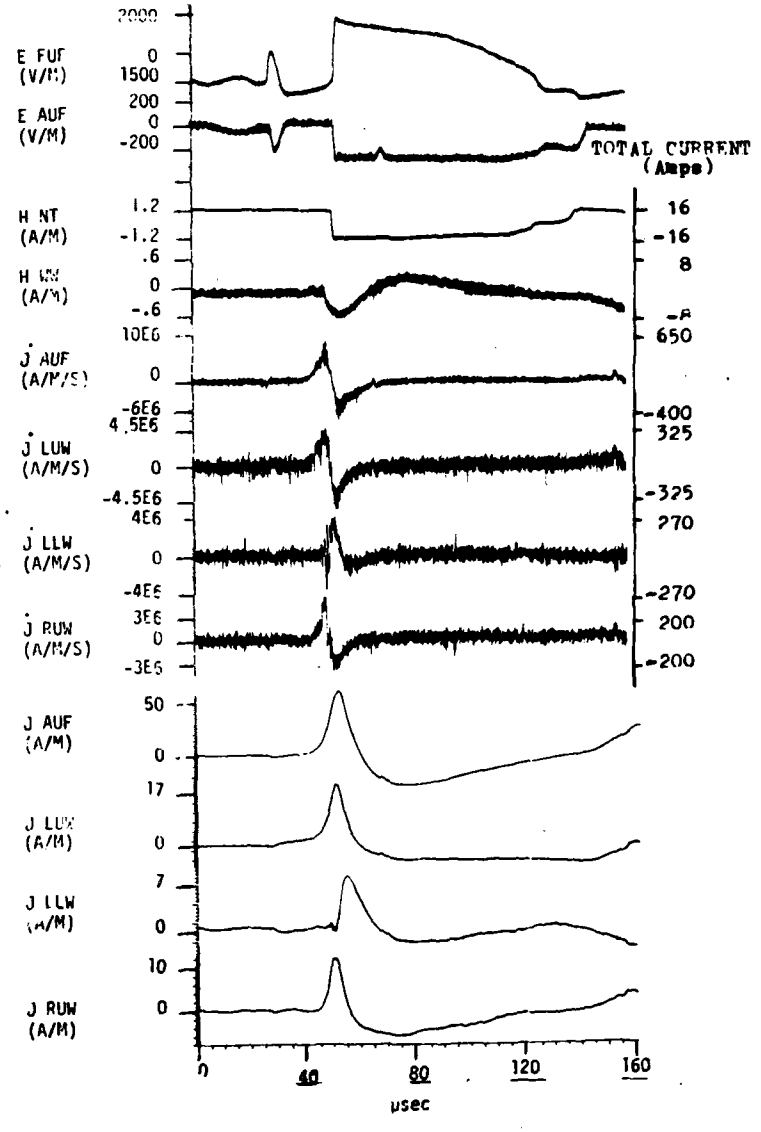

Figure 26 164 μsec

Additionally the risetimes of the unsaturated sensors were looked at with several 164 μsec windows. Some typical pulses are shown in figures 27 and 28. Figure 27 represents an expanded E AUF pulse that was used in the risetime calculations. Figure 28 shows an expanded H WW pulse that yielded a risetime of 711 nanoseconds. Table IX shows the risetimes and magnitude changes over the risetimes for unsaturated pulses in various sensors. The maximum and minimum risetimes were 6.00 μsec and .19 μsec respectively. This minimum risetime is not accurate because pulses faster than about 350 μsec could not be resolved due to the limited bandwidth. Table X shows a summary of some of the more important features of the two flashes.

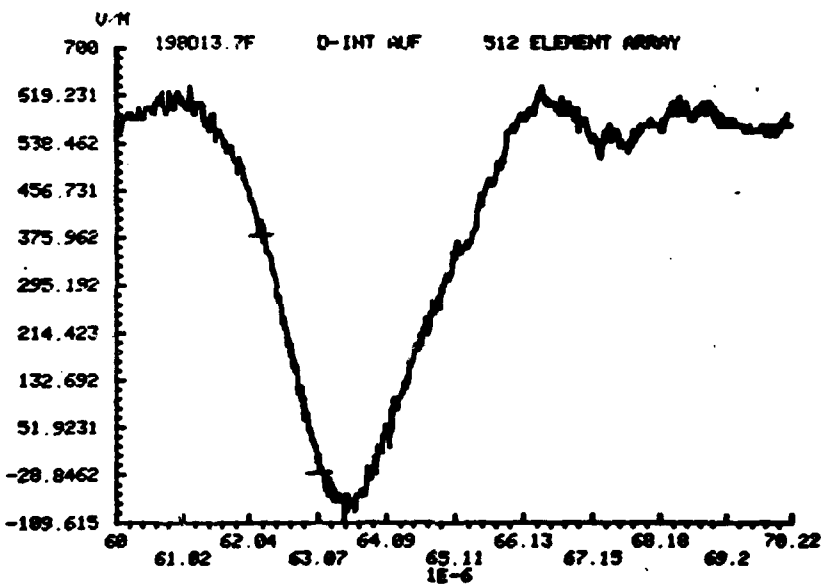

Figure 27 Expanded E AUF waveform for risetime calculation

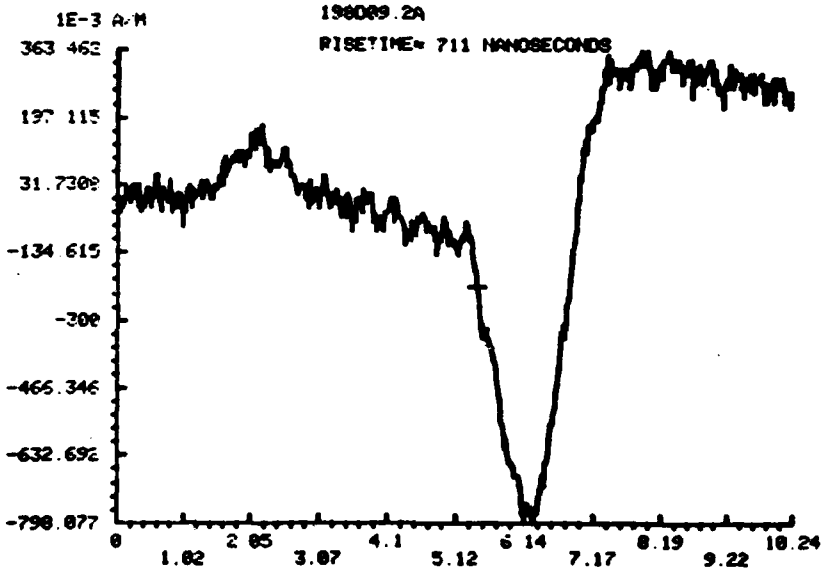

Figure 28 Expanded H WW Waveform for risetime calculations

Pulse #	1	2	3	4	5	6	7	8	9	10
J AUF	.19	1.10	.21	.63	.35	3.80	6.00	.35	1.00	.38
J LUW	.50	.99	.20	-	.40	2.80	5.00	.22	.90	.22
H WW	1.00	2.00	-	.71	-	6.00	3.50	-	-	1.40
E AUF	-	-	-	-	-	-	-	.95	1.40	1.00
J AUF A/M/μS	4.8	4.5	1.9	3.17	1.1	10.7	4.16	6.4	4.0	10.5
J LUW A/M/μS	1.2	2.5	7.5	-	1.25	2.6	1.16	5.5	2.5	5.5
H WW A/M/μS	.2	.35	-	1.4	-	.08	.09	-	-	.82
E AUF V/M/μS	-	-	-	-	-	-	-	420	360	700

Risetimes (Microseconds)

Magnitude Change Over Risetime

Table IX Risetimes for 17 July

	17 July	26 August
Flash Duration	295 msec	460 msec
Maximum Pulse Repetition Rate	10^4 pulses/sec	10^4 pulses/sec
Total Number of pulses	150-200	200-300
Maximum Uniform Current flow in a single pulse	650 A	3 KA
Maximum Electric Field change in a pulse	2000 V/m (Saturation level)	2000,000 V/m
Maximum Magnetic Field Change in a pulse	1.8 A/m (Saturation level)	1.8 A/M (Saturation level)
Risetime	Max: 6 μsec	Max: 3 μsec
	Min: about 20% below BW limit of 250 nsec	Min: about 25% below BW limit of 250 nsec
Continuing Current	50 A	———

Table X Comparison of Characteristics

Comparison With Other Data

General

The purpose of this chapter is to compare the results of these two strikes with past experimental data that has been recorded by Gunn (Ref. 2), Fitzgerald (Ref. 3), Nanevicz et. al. (Ref. 4), the French Transall data (Ref. 5), NASA (Ref. 6 and Ref. 7) and Rustan, et. al. (Ref. 8). By comparing the data with previous results, it is possible to improve our understanding of our own data.

Gunn

The primary feature of the data collected by Gunn (Ref. 2) was the observation that the electric field just before the flash was on the order of 300,000 V/M. This field level is comparable to the largest electric field change seen on the 26 August of 200,000 V/M but since no electrostatic field was measured an exact comparison is not possible.

Fitzgerald

The main features of Fitzgerald's data (Ref. 3) relates to currents and $\frac{dI}{dt}$. His peak values correspond well with the 26 August data with the following exceptions. The peak currents reported by Fitzgerald are in the right wing tip and the vertical stabilizer and are on order of magnitude higher than those obtained here. Since he drew his data from over 50 strikes, we can consider his conclusions from the peak value of the 26 August strike of

moderate intensity and the 17 July strike was of low intensity.

Nanevicz et. al.

The data presented by Nanevicz et. al. (Ref. 4) features a maximum E field change of about 50 KV/M and an average time between pulse of 17 msec. The pulses are much further apart in the Nanevicz data and the pulses show no exponential decay. This is possibly due to the fact that their aircraft was not in cloud and hence the triboelectric charging rate was quite low. This meant that the aircraft needed longer to recharge. No decay was probably seen because the charge in the cloud was not significantly altered during the flash.

French Transall Data

The French Transall data (Ref. 5), more specifically the type 1 flashes encountered correlate well with the data in this thesis. However all the French direct strike data showed a continuing current. Even though no continuing current was evident on our 26 August strike, it was probably there but no concrete verification could be found.

NASA Data

NASA reports (Ref. 6) present several interesting aspects to their data, some of which are applicable to the results in this thesis. A good comparison can be made by selecting one of NASA's strike pulses that is characterized by a peak E field on the order of 380,000

V/M versus this thesis peak of 200,000 V/M change. Their H field was about 5.6 A/M. Our value was estimated at about 3 A/M. There is also a good agreement in E/H ratio. Also the value of 88 A presented in the NASA data is much smaller than our peak values of 650 A and 3 KA.

AFWAL

The preliminary results of Rustan et. al. (Ref. 8) are most applicable to this data. In this report the 26 August direct strike is analyzed. The preliminary conclusions made by Rustan et. al. are in agreement with those in this thesis.

Model

Based on the data collected from these two strikes, a theoretical model can be developed of the physical processes involved in a direct lightning strike to an aircraft. This model is for a cloud-to-aircraft type strike where the only charges involved in the strike are in a cloud charge center and the charge on the aircraft. The large number of pulses (300) and duration of pulses (several microseconds) in the data are not characteristic of typical wideband electric field records of cloud-to-ground or intracloud lightning flashes. In addition since there is no evidence in the data of continued leader propagation after contacting the aircraft, there is no electrical connection with either ground or another charge center.

The direct strike starts with the formation of a leader either from the aircraft or from the cloud. The distance between the cloud charge center and the aircraft is formed and a transfer of whatever charge is on the aircraft to the oppositely charged cloud center takes place in a few microseconds. The amount of charge transfer is the total amount of charge that is being held by the aircraft and any streamers that may be propagating from it. This corresponds to a peak current of several hundred to a few kiloamps depending upon how much charge is on the aircraft. Once the charge on the aircraft has been neutralized, the aircraft begins to recharge. This occurs by tri-

boelectric charging from the frictional effect of snow and ice and the glazing effect of supercooled cloud droplets (Ref. 18 p. 291). If charge in the cloud pocket still exists, charge will not only deposit on the aircraft but will also flow up the channel directly to the cloud charge center. This will neutralize the charges in the cloud of opposite polarity. This time instead of an abrupt charge transfer, the current flows as a uniform continuing current on the order of 50 A until either the cloud charge center is neutralized or the channel finds another concentrated charge pocket in the cloud. When this occurs the transfer of charge process starts over and over again until either no more cloud charge pockets can be found or the channel starts to de-ionize.

Several characteristics of the data support this hypothesis for a direct strike to the aircraft. First the electric field sensor E LWT that was calibrated on 26 August for large E-field changes show an overall trend of exponential decay throughout the flash. This decay can be explained as the charge loss in the cloud over the time period of the strike. Each time a pocket of charge in the cloud is neutralized by the aircraft charge, the electric field will decrease by a proportional amount.

Another interesting point that the data shows is that the triboelectric charging rate is higher for sleet, snow, or ice than for rain. Gunn (Ref. 2) and Fitzgerald

(Ref. 3) point out that precipitation static rarely is reported in rain. For the 26 August strike, the aircraft was flying in mixed precipitation. On 17 July the aircraft was flying in rain. The maximum currents recorded for each day correspond to the maximum charge on the aircraft, and the large current pulses for each flash are about the same distance apart (8-200 μs), Therefore the charge buildup between aircraft discharges depends only on the charging rate. The 26 August strike then has the higher triboelectric charging rate which must therefore be due to the aircraft flying in an environment that enabled more charging of the aircraft.

The charge center of the cloud must be made up of many small pockets of charge that are of the same polarity and grouped together to form one of the three observed regions of charge in a cloud. If each one of these pockets is represented as a large current pulse seen in the J sensors then only about ten of these pockets actually takes part in an aircraft to cloud strike.

If the assumption that the aircraft charge is neutralized each time the channel comes in contact with a new pocket of charge in the cloud then the following conclusion seems likely. Plumer (Ref. 17) and Shaeffer (Ref. 12) state that an aircraft can hold only about 100 μC to several millicoulombs of charge. Furthermore the highest charging rate observed is on the order of 3 A (Ref. 13). These values do not agree with the measured data reported

on here. This data shows aircraft charge on the order of 30 to 50 mC and a charging rate on the order of 400 A. This is a large discrepancy but probably can be explained by the fact that no one else has yet measured the current charging the aircraft in a large E-field with an external source of free charge available to an aircraft that has just been neutralized. All previous values are either based on calculations, (Ref. 13), laboratory tests (Ref. 12), or the aircraft being gradually introduced into a region where triboelectric charging will occur. In addition Clifford (Ref. 13) has inferred that since calculations yield a charge density as high as 0.2 coulombs per cc of super cooled water, a single one-μ supercooled water droplet can impart enough charge on the aircraft by impact so as to produce corona from its surface (70,000 V/M). In addition Clifford cites Nanevicz's for a normal raindrop concentration of 5×10^4 per cubic meter in thunderstorms. He then calculates a charging rate on the order of hundreds of amperes fro an aircraft flying at 100 meters per second. This is about the observed rate during the flashes in this thesis.

Summary

There are some important conclusions that can be derived from this data, primarily the notion of a clouf-to-aircraft triggered strike. This has never been addressed before in the literature. Several authors (Ref. 17, Ref. 3, and Ref. 4) indicate that an aircraft is involved in the lightning process as either in the path between an intracloud or cloud to ground discharge or else experiencing a static discharge. Neither of these possibilities is indicated from the data. The presence of a leader, either from the cloud or from the aircraft rules out a static discharge and the lack of continued leader propagation rules out the other two natural lightning discharges. Except the case of an intracloud discharge where the leader is caused by simultaneous propagation of leaders from the charge centers which meet at the aircraft.

The indication that the aircraft or aircraft and streamers can hold a charge on the order of 30-50 mC is also new. Previous results have indicated that an aircraft can only hold a charge on the order of several hundred microcoulombs to few millicoulombs. Additionally, the indication that the aircraft can charge at the rate of hundreds of amperes is a new concept, at least from the experimental point of view.

Continuing currents on the order of 50 A were experimentally derived. The majority of activity that occurred in the flashes was in the first 30-40 msec with a discrete pulse train made up of around 100 pulses. Total flash duration is indicated on the order of 300 msec. Rise-times for most of the pulses were around one microsecond. Transients were induced on internal wires with the wing wires showing quite a bit more activity than the fuselage wire. There doesn't seem to be any direct correlation between magnitude measured on any of the sensors and the magnitude of transients induced on either of the internal wires.

The transfers of charge from the aircraft during the flash neutralizes the charge in the cloud reducing the external field considerably. Electric field changes on the order of 200 KV/M were seen. Magnetic field changes on the order of 3 A/M were extrapolated and several current pulses on the order of hundreds of amperes to a few kiloamperes were experienced. These current pulses lasted from several to tens of microseconds. These are some of the first extensive records of correlated E, H and $\dot{J}$ waveforms and hopefully they have and will continue to contribute to an advancement of the state-of-the-art in this area of research.

Several recommendations are made as a result of the work done in this thesis. These recommendations mainly apply to those who intend to do future research in the area of airborne lightning characterization.

There were several problems with the instrumentation. Assumptions were made that need to be verified. A $\dot{J}$ FUF semsor should be installed so as to compare the percentage of current that flowed through the rear fuselage to the front fuselage. In this thesis both were assumed to be equal. However the French (Ref. 5) have published results indicating that current entering the nose is not equal to that leaving the tail. Another problem is in estimating the amount of current that is flowing through the fuselage or wings. The $\dot{J}$ sensors are only in one location and only measure a portion of the current that flows. Then calculations by Burroughs (Ref. 16) computer program has been used to determine the uniform current flow. This technique assumes current flow across the entire fuselage or wing and does not address the point of an attachment at some point other than the nose. Several other techniques seem to be more useful and accurate. First a ground test with applied currents at several attachment points with waveforms similar to those presented here. Another possibility is to have another aircraft or series of ground stations to measure the current via H-field measurements. This may also address the question of whether or not the current flowing in the channel also

completely flows through the aircraft or whether only a portion flows through the aircraft itself. If ground stations could be used, a better understanding could be reached as to the type of flash along with a possible map of VHF source locations as the one introduced by Rustan et. al. (Ref. 19). Another instrumentation problem was obviously the saturation levels. This was mainly due to the fact that most of the aircraft sensors were not calibrated for recording direct strike data but rather a wide variety of near and far-field data. If the aircraft sensors were calibrated for direct strikes then more accurate waveforms would be measured. Several additions to the instrumentation are also proposed. Field mills similar to those used by Gunn (Ref. 2), Fitzgerald (Ref. 3), Nanevicz et. al. (Ref. 4) would be helpful in three ways: (1) the charge of the aircraft could be determined. (2) The three components (Ex, Ey, Ez) of the electric field could be measured to give a more accurate representation of the charge concentration which is present when lightning occurs. Also these components could be applied to Pierce (Ref. 11) criteria for triggered lightning so as to see if any of these components would yield the suitable values established by Pierce. Another addition should be J sensors with DC and low frequency response. This would establish an accurate means of measuring the con-

tinuing current rather than estimating from burn marks (which may or may not exist). Also if a low pass filter is used, the streamer propagation (if it exists) could be followed after the initial attachment takes place.

Additional interior wiring needs to be monitored for a response to the flash. This would probably be best accomplished by ground testing once a suitable model is developed.

The recommendation most important is the need for continuing research and collection of airborne lightning data. Only two flashes are presented here, not nearly enough to draw steadfast conclusions from as to or worst case or even typical lightning strikes.

Bibliography

1. Clifford, D.W. "Aircraft mishap experience from Atmospheric Electricity, NATO AGARD Lecture Series No. 110, Paper no. 2 (June 1980).

2. Gunn, R. "Electric Field Intensity Inside of Natural Clouds," J. Appl. Phys., Vol. 19, pp. 481-484, May 1948.

3. Fitzgerald, D.R. "Aircraft and Rocket Triggered Natural Lightning Discharges," Lightning and Static Electricity Conference, AFAL Rep. TR-68-290, Part II, (Dec. 1968).

4. Nanevicz, J.E., Adamo, R.C., and Bly, R.T., "Airborne Measurements of Electromagnetic Environment Near Thunderstorm cells (TRIP-76)," Stanford Research Institute Final Report, Air Force (FDL) Contract NAS 9-15101 (March 1977).

5. Centre D/Essais Aeronautique De Toulouse, "Mesure Des Characteristiques De La Foudre En Altitude," Essais No. 76/650000P.4et Final (July 1979).

6. Pitts, F.L. "Electromagnetic Measurement of Lightning Strikes to Aircraft," AIAA 19th Aerospace Sciences Meeting, Paper No. 81-0083, (January 1981).

7. Pitts F.L., and Trost, T.F. "Analysis of Electromagnetic Fields on an F-106B Aircraft During Lightning Strikes" NASA Technical Report.

8. Rustan, P.L., Kuhlman B.P., DuBro, G.A., Reaver, M.J., Risky, M.P., and Serrano, A.V., "Correlated Airborne and Ground Measurements of Lightning," Intl. Aerospace Conference on Lightning and Static Electricity, Oxford, England, 23-25 March 1982.

9. Baum, R.K., "Airborne Lightning Characteristics," FAA/NASA/FIT Symposium on Lightning Technology, Hampton, VA. 22-24 April 1980.

10. Rustan, P.L., Kuhlman, B.P., DuBro, G.A., Reazer, M.J., Risley, M.D., and Serrano, A.V. "Correlated Airborne and Ground Measurements of Lightning" AF Technical Report, unpublished.

11. Pierce, E.T., "Triggered Lightning and Its Application to Rockets and Aircraft," 1972 Lightning and Static Electricity Conference, USAF Rep. AFAL-TR-72-325 (December 1972).

12. Shaeffer, J.F., "Aircraft Initiation of Lightning," 1972 Lightning and Static Electricity Conference USAF Rep. AFAL-TR-72-325 (December 1972).

13. Clifford D. W. "Another Look At Acft-triggered Lightning" FAA/NASA/FA Symposium on Lightning Technology, Hampton VA. (April 1980).

14. Clifford D.W., and Kasemir, H.W., "Triggered Lightning" to be published in IEEE Trans. on Electromagnetic Compatability Part I, Special Issue on Lightning - Its Interaction with Acft (May 1982).

15. Baum, C.E., "Electromagnetic Pulse Sensor Handbook" EMP Measurement 1-1 (June 1971).

16. Burroughs, B.J.C., "Absolute Calibration of $\dot{B}$ and $\dot{J}$ sensors on FY 80 WC130 Aircraft" USAF contract No. F61708-81-M0140 (June 1981).

17. Fisher, F.A., and Plumer, J.A., "Lightning Protection of Aircraft" NASA Reference Publication 1008 (Oct. 1977).

18. Chalmers, J.A. Atmospheric Electricity, Pergamon Press Second Ed. Oxford (1967).

19. Rustan, P.L., Kulman, M.A., Childers, D.G., Beasley, W.H., and Lennon, C.L., "Lightning Source Locations from VHF Radiation Data For a Flash at Kennedy Space Center," J. Geophys. Res., 85, 4893-4903, Sept. 1980.

20. Brook, M., Holmes, C.R., and Moore, C.B., "Lightning and Rockets: Some Implications of the Apollo 12 Lightning Event," Naval Research Reviews, April 1970.

Vita

Jeffrey S. Schowalter was born in Milwaukee, Wisconsin. He attended Hartford Union High School. In 1978, he married the former Laura Van Gilder of Menomonee Falls, Wisconsin. Later that year he graduated from the University of Wisconsin-Milwaukee with a B.A. and was commissioned after attendance at the Officer Training School. He was subsequently assigned as a Weather forecaster at Langley AFB, Virginia. In 1979 he was accepted into the undergraduate EE degree conversion program at AFIT. While attending AFIT, his two sons Adam and Ryan were born. In 1981, he received his B.S.E.E. degree from AFIT and was thereupon extended to complete his master's degree.

Permanent address: 1157 Forest Court, Hubertus, Wisconsin 53033.

UNCLASSIFIED

SECURITY CLASSIFICATION OF THIS PAGE (When Data Entered)

REPORT DOCUMENTATION PAGE	READ INSTRUCTIONS BEFORE COMPLETING FORM
1. REPORT NUMBER: AFIT/[illegible]/EE/82J-12	2. GOVT ACCESSION NO. [illegible] 3. RECIPIENT'S CATALOG NUMBER
4. TITLE (and Subtitle): DIRECT LIGHTNING STRIKES TO AIRCRAFT	5. TYPE OF REPORT & PERIOD COVERED: MS Thesis
	6. PERFORMING ORG. REPORT NUMBER
7. AUTHOR(s): Jeffrey S. Schowalter, 1st Lt USAF	8. CONTRACT OR GRANT NUMBER(s)
9. PERFORMING ORGANIZATION NAME AND ADDRESS: Air Force Institute of Technology (AFIT-EN) Wright-Patterson AFB, Ohio 45433	10. PROGRAM ELEMENT, PROJECT, TASK AREA & WORK UNIT NUMBERS
11. CONTROLLING OFFICE NAME AND ADDRESS: Flight Dynamics Laboratory (AFWAL/FIESL) Wright Aeronautical Laboratories Wright-Patterson AFB, Ohio 45433	12. REPORT DATE: June 1982
	13. NUMBER OF PAGES: 128
14. MONITORING AGENCY NAME & ADDRESS (if different from Controlling Office)	15. SECURITY CLASS. (of this report): Unclassified
	15a. DECLASSIFICATION/DOWNGRADING SCHEDULE

16. DISTRIBUTION STATEMENT (of this Report)

Approved for public release; distribution unlimited

17. DISTRIBUTION STATEMENT (of the abstract entered in Block 20, if different from Report)

18. SUPPLEMENTARY NOTES

APPROVED FOR PUBLIC RELEASE: IAW AFR 190-17

LYNN E. WOLAVER
Dean for Research and Professional Development

AIR FORCE INSTITUTE OF TECHNOLOGY (ATC)
WRIGHT-PATTERSON AFB, OH 45433

23 JUL 1982

19. KEY WORDS (Continue on reverse side if necessary and identify by block number)

Lightning
Direct Strike
Aircraft
Electromagnetic Compatability
Lightning Strike
Airborne Lightning
Triggered Lightning

20. ABSTRACT (Continue on reverse side if necessary and identify by block number)

Two direct strikes to a WC-130 aircraft equipped with eleven electromagnetic field sensors were recorded during the summer of 1981.

An analysis of the data shows both strikes exhibit a train of discrete pulses which can be correlated in most of the eleven sensors. The flashes lasted 295 and 460 msec and were characterized by an initial active period of about 40 msec where most of the activity occurred. In both flashes the majority of the curren

DD FORM 1 JAN 73 1473 EDITION OF 1 NOV 65 IS OBSOLETE

UNCLASSIFIED

SECURITY CLASSIFICATION OF THIS PAGE (When Data Entered)

flow was along the fuselage with peak currents estimated at 3 KA in one flash and 650 A in the other flash. A continuing current of an estimated 50 A was evident in only one strike. The electric field sensors recorded a maximum change of 200,000 V/M. In one case the leader appears to propagate from the cloud to the aircraft. In the other case leader appears to initiate from the aircraft. No evidences were found of continued leader propagation after aircraft contact, thus suggesting the occurrence of a cloud-to-aircraft lightning flash.

Transients were measured on internal aircraft wires on the order of 40 mV. Most of the transient pulses were induced on a wire which ran from wing to wing.

END

DATE
FILMED

9 -82

DTIC